GE NUCLEAR ENERGY

GENE Report No. B13 - 01739 - 25
DRF No. B13-01739
Class III

Core Shroud Repair
270° Tie Rod Assembly Assessment
(Non Proprietary Version)

Prepared for
Niagara Mohawk Power Corporation
Nine Mile Point Nuclear Station, Unit 1

Prepared by
GE Nuclear Energy
Reactor Modification Services

IMPORTANT NOTICE REGARDING CONTENTS OF THIS REPORT

Please Read Carefully

The only undertakings of the General Electric Company (GE) respecting information in this document are contained in the contract between GE and NMPC and nothing contained in this document shall be construed as changing the contract. The use of this information by anyone other than NMPC, or for any purpose other than that for which it is intended for, is not authorized; and with respect to any unauthorized use, GE makes no representation or warranty, express or implied, and assumes no liability as to the completeness, accuracy, or usefulness of the information contained in this document, or that its use may not infringe privately owned rights.

GE NUCLEAR ENERGY

GENE Report No. B13 - 01739 - 25
DRF No. B13-01739
Class III

Core Shroud Repair
270° Tie Rod Assembly Assessment
(Non Proprietary Version)

April, 1996

Prepared by: T E Gleason 4-29-96
T.E. Gleason, Principal Engineer
Reactor Modification Services

Approved by: S Ranganath 4/29/96.
S. Ranganath, Engineering Fellow
GE Nuclear Engineering

TABLE OF CONTENTS

TABLE OF CONTENTS

1. INTRODUCTION AND SUMMARY

Following the installation of the core shroud repair at Nine Mile Point 1 (NMP1), a visual inspection of the as-installed hardware showed that the lower spring wedge of the 270º tie rod assembly was bearing against a recirculation nozzle weld instead of the vessel. The resulting contact area appeared to be approximately 2/3 of the full wedge area. This was evaluated by GE Nuclear Energy (GE) and Niagara Mohawk Power Corporation (NMPC) and found to be acceptable 'as is'. Subsequently the NRC reviewed the analysis and concluded in the safety evaluation that the requirements of the shroud repair were met.

Susequent reviews of the videotapes of the 270º tie rod assembly and 3D Computer Aided Drafting (CAD) layouts have shown that the actual wedge contact area is less than the originally estimated 2/3 and may be as low as 9% of the full wedge area. Also, the wedge contact is on an inclined surface of the nozzle. Figure 1-1 and 1-2 show the 270º tie rod assembly and the as-installed configuration. Although both GE and NMPC completed evaluations to determine that the shroud repair function is still maintained, since this was a change from the assumptions of the previous analysis, NMPC notified the NRC. The purpose of this report is to provide a technical evaluation of the adequacy of the 'as-installed' condition of the 270º tie rod assembly and confirm the effectiveness of the repair.

Section 2 of this report describes the background on the 270º tie rod issue. The chronology of events that led to the finding, the analytical basis for the earlier field deviation, the determination of the as-installed condition, including the videotape and CAD review, the new estimate of the contact area, the related operability concerns and the effect of displacements are discussed in Section 2. The applied loading resulting from the partial wedge contact on an inclined slope of the nozzle is described in Section 3. The structural analysis and safety assessment is described in Section 4. The structural assessment considers a series of increasingly conservative postulates on the condition of the 270º tie rod assembly. First (in Section 4.1) it is assumed that there is point contact of one edge of the wedge on the nozzle (but no slipping), resulting in a twisting moment on the lower spring and it is shown that the stresses in the hardware are within the specified limits. In Section 4.2, point contact is assumed as before, but

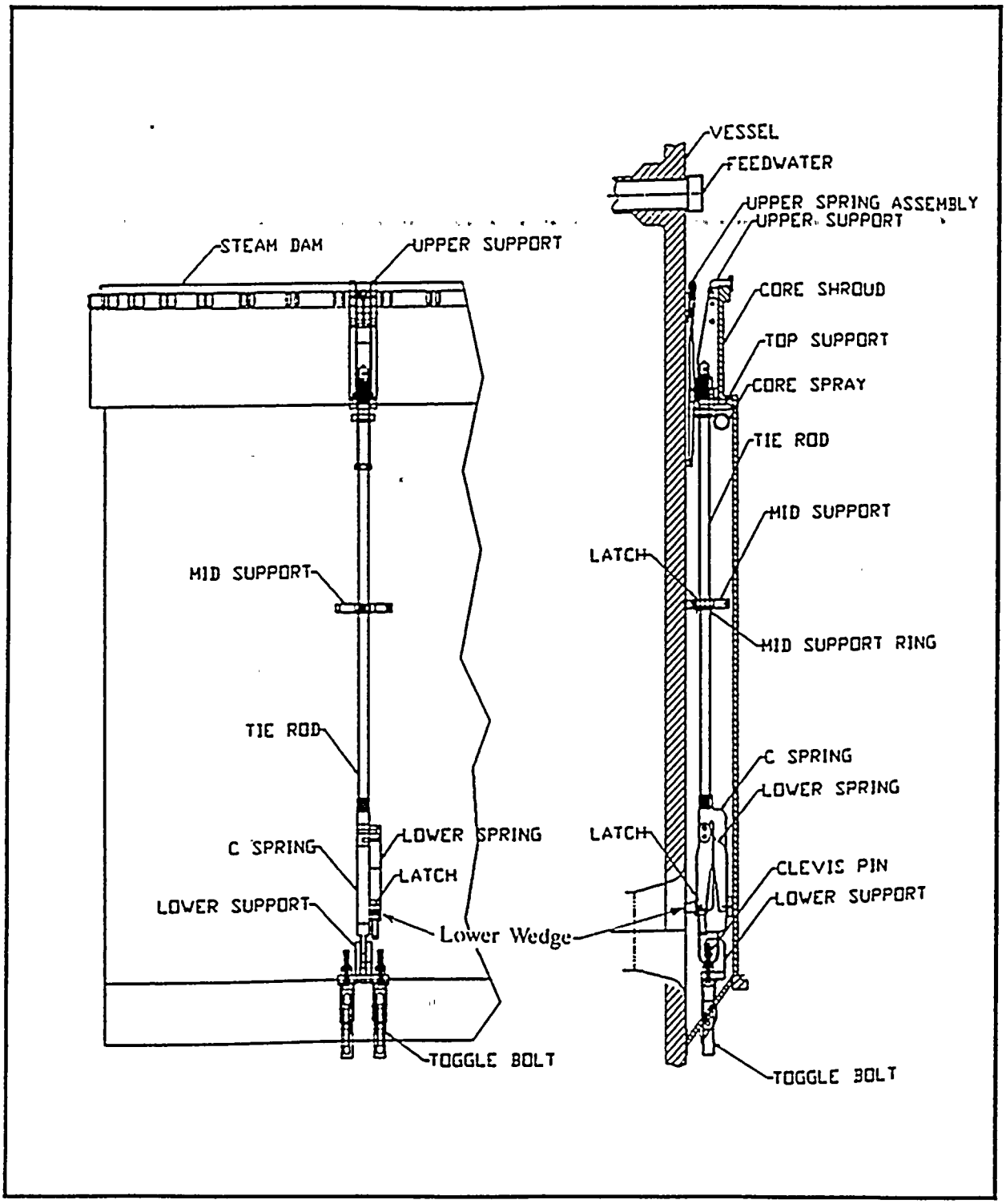

Figure 1.1
Core Shroud Stabilizer

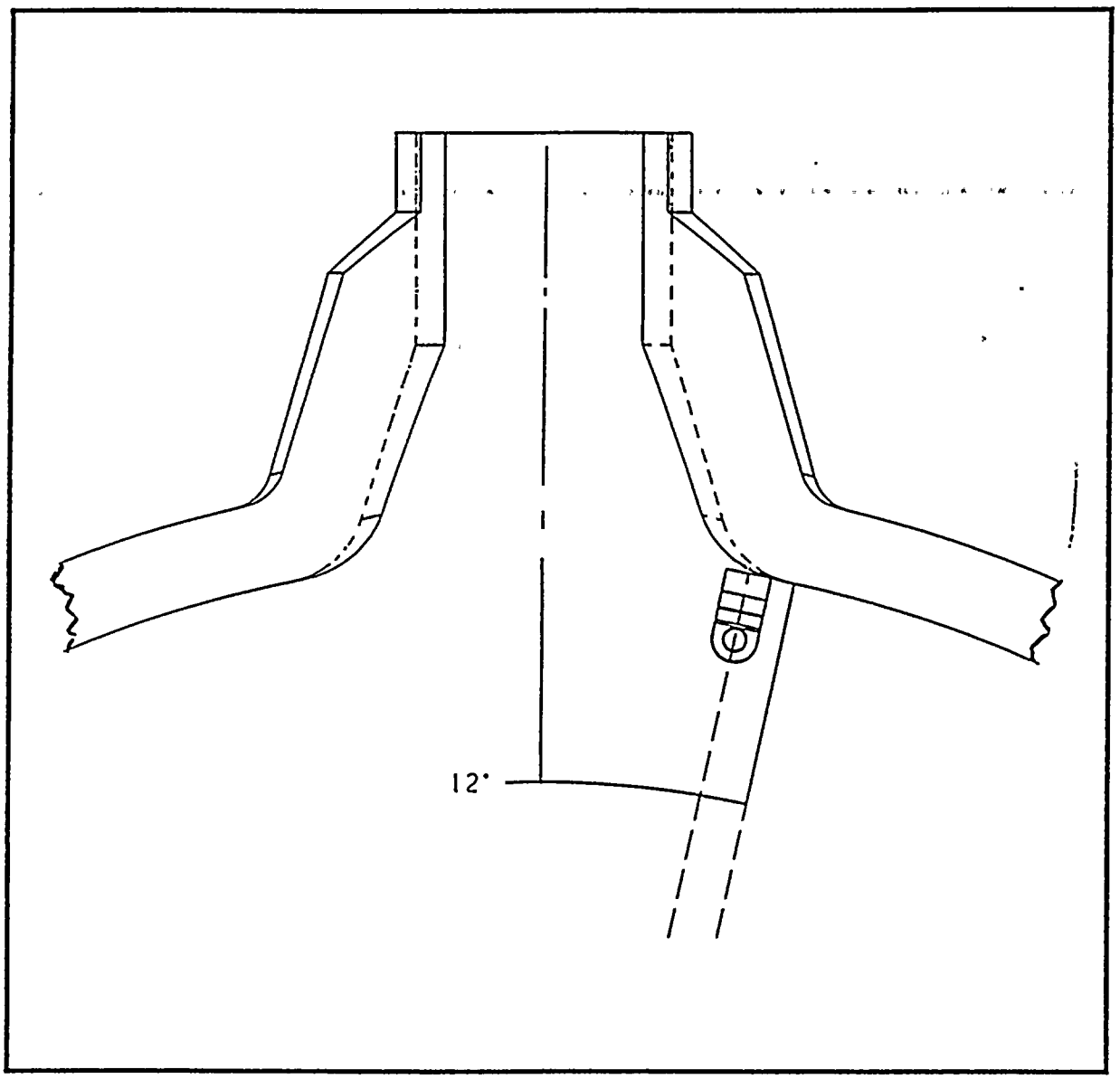

Figure 1.2
Top View of Lower Wedge on Nozzle

slipping is also allowed. This applies a lateral load on the lower spring that tends to bend the pin connecting the C-spring to the lower spring. As described in Section 2, it is estimated that the contact angle could range from 2º to 8º depending on the tolerances. In order to account for potential uncertainties in the 8º estimate, it was assumed conservatively that the contact point is one inch away from the expected location. This corresponds to a contact on a slope of 22º into the nozzle. It is shown that even with contact occurring on a 22º-slope surface, the lateral force will not lead to failure of the pin. In Section 4.3, it is assumed that the lower spring is totally ineffective (no resistance to lateral motion of the shroud) and it is shown that even in this condition, the lateral displacements are not high enough to impede control rod insertion. Other safety considerations such as the potential for flow induced vibrations (FIV) and the probability of 360° through wall shroud cracking are addressed in Section 5. Details of the hardware stress analysis, vessel analysis including bearing stress evaluation, description of the seismic model and documentation of the friction factors are provided in the appendices.

Based on the evaluations described here, it is concluded that the as-installed condition of the 270º tie rod assembly is acceptable and that all safety functions provided by the shroud repair are maintained.

2. BACKGROUND

2.1 Chronology of Events

Following the core shroud repair installation in March 1995, NMPC provided the NRC with a description and evaluation of three (3) deviations associated with the NMP1 core shroud repair installation discovered after final inspection The third deviation concerned the 270° azimuthal tie rod assembly wherein the lower spring and wedge was found to be bearing against a recirculation nozzle weld. The March 23, 1995, letter stated that the contact area between the lower wedge and the reactor pressure vessel wall is approximately 2/3 of the wedge area. The March 23, 1995, report from NMPC also identified 10 percent of the wedge contact area as an acceptable minimum area for bearing stress. The March 23, 1995, letter submitted analysis that evaluated the as-found condition and concluded that the deviation was acceptable. The NRC staff reviewed the analysis of this deviation and concluded in the NRC Safety Evaluation Report (SER) for the NMP1 core shroud repair modification dated March 31, 1995, that all existing analysis remain valid.

The H6A deviation discussed in the March 23, 1995, letter was only approved for use through the next refuel outage by the NRC SER. NMPC nuclear engineering was evaluating corrective actions for this deviation and also evaluating the long-term implications of the 270° tie rod location deviation. During the course of those evaluations, all of the available inspection tapes of the shroud repair installed hardware were reviewed by NMPC nuclear engineering. One of the inspection tapes showed a reverse angle perspective which appeared to indicate a different contact condition than was previously described. Figure 2.1 is the view most likely used to describe the previous condition. Figure 2.2 is a reverse angle view.

Since GE Nuclear Energy was the supplier and installer of the shroud repair hardware and had dispositioned the original evaluation in March 1995, NMPC nuclear engineering requested that GE Nuclear Energy evaluate the videotape in question and apply 3D Computer Aided Drafting (CAD) layouts of the lower

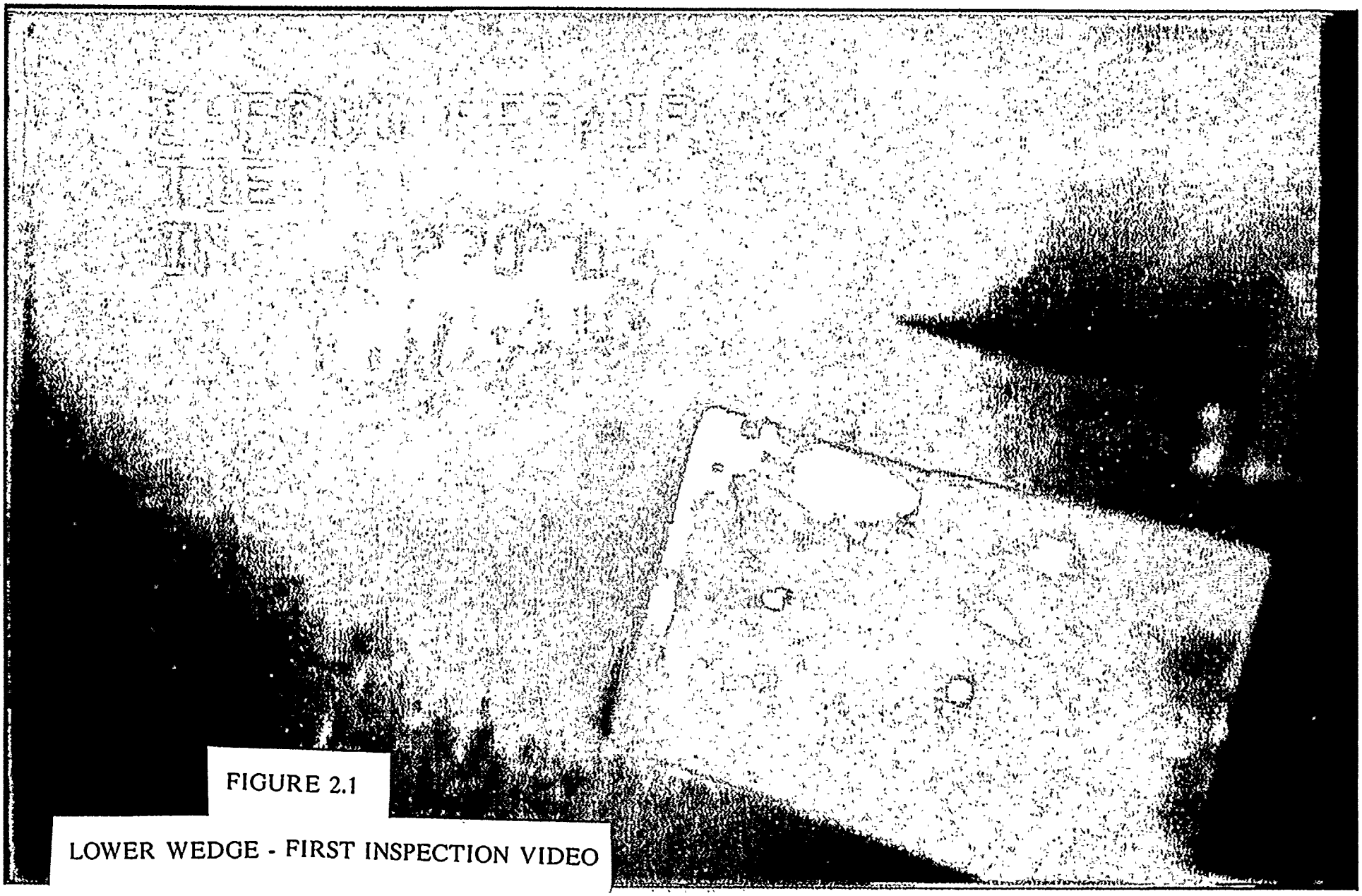

FIGURE 2.1

LOWER WEDGE - FIRST INSPECTION VIDEO

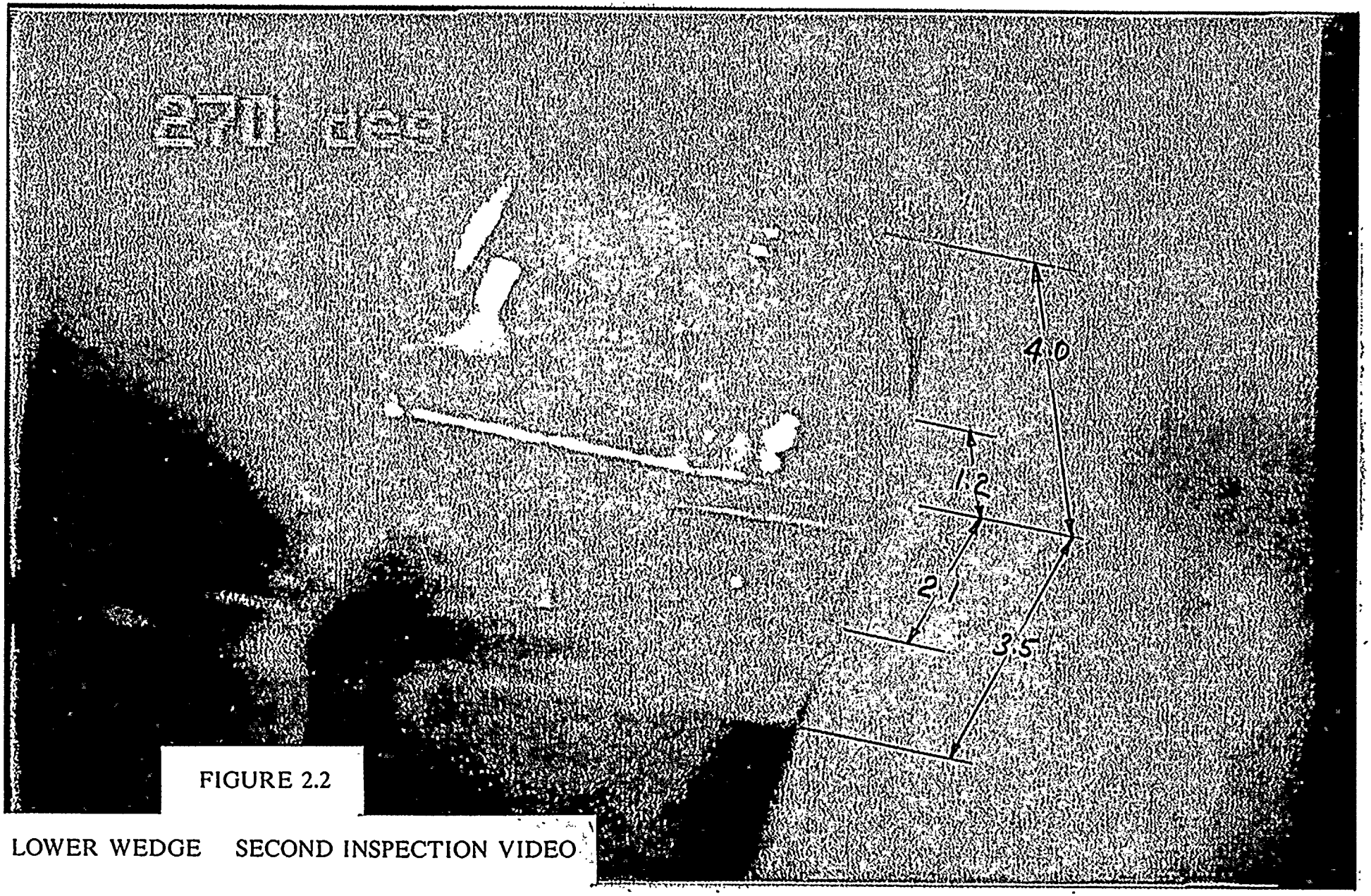

FIGURE 2.2

LOWER WEDGE SECOND INSPECTION VIDEO

wedge contact to help clarify the location. On March 21, 1996, GE submitted to NMPC, documentation that indicated that the actual area of contact is on the blend radius of the recirculation nozzle, and is making contact on an inclined surface estimated to be 2° to 3°. The wedge contact area appeared to be over a smaller area than indicated in the original GE disposition. Because the lower wedge contact was now presumed to be on the nozzle radius inclined surface and because the contact area was less than the area assumed in the original disposition, NMPC initiated an internal Deviation Event Report on March 22, 1996, to address operability, reportability, and corrective action.

NMPC notified the NRC on March 22, 1996, at 20:16 EST under provisions of 10CFR50.72(b)(1)(ii)(B), (Outside Design Basis). NMP1 was operating at 100 percent rated power at the time of notification. The notification was made because of a discrepancy in the installed 270° azimuthal location shroud repair stabilizer assembly lower spring component different from that in the 10CFR50.55a shroud repair submitted and NRC SER. The location of this component had been reviewed and approved by the NRC with 2/3 of the lower spring wedge surface area in contact with one of the reactor recirculation suction nozzles. The actual location was determined to contact the recirculation nozzle on the blend radius with a reduced contact area of approximately 9 percent of the available contact area.

NMPC submitted Licensee Event Report (LER), LER 96-02 to the NRC April 22, 1996. This LER concludes that the design basis function of this component was maintained, but the location was not as described in the NRC SER. The root cause of this event is a post-installation inspection deficiency due to personnel error. The cause is described in detail in the LER.

2.2 Determination of the As-Installed Condition

Additional efforts were made to characterize the contact location and to determine any affects on the initial FDDR disposition. The concern is that the contact may be bearing on an inclined surface which further relies on friction

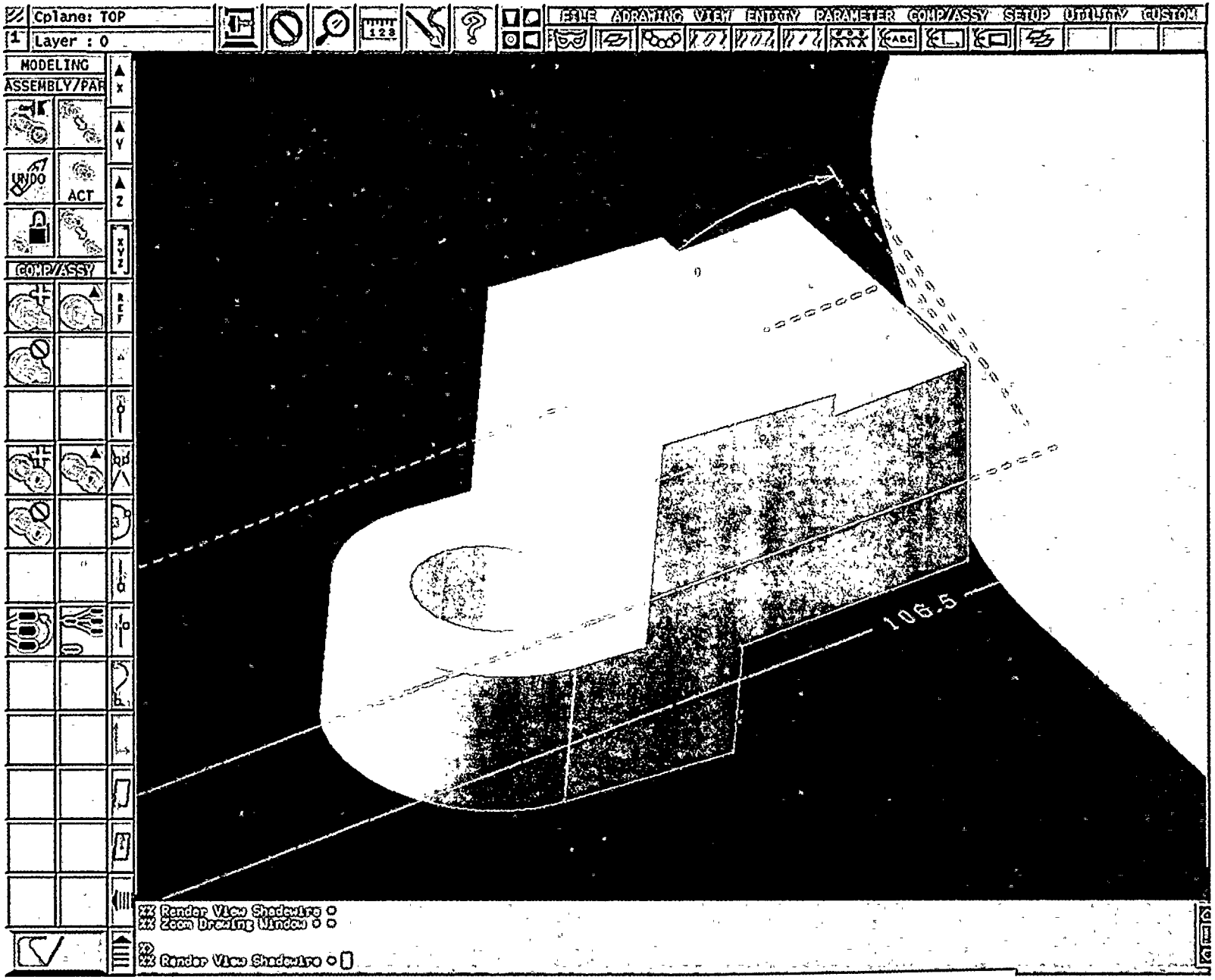

FIGURE 2.3 LOWER WEDGE AND NOZZLE

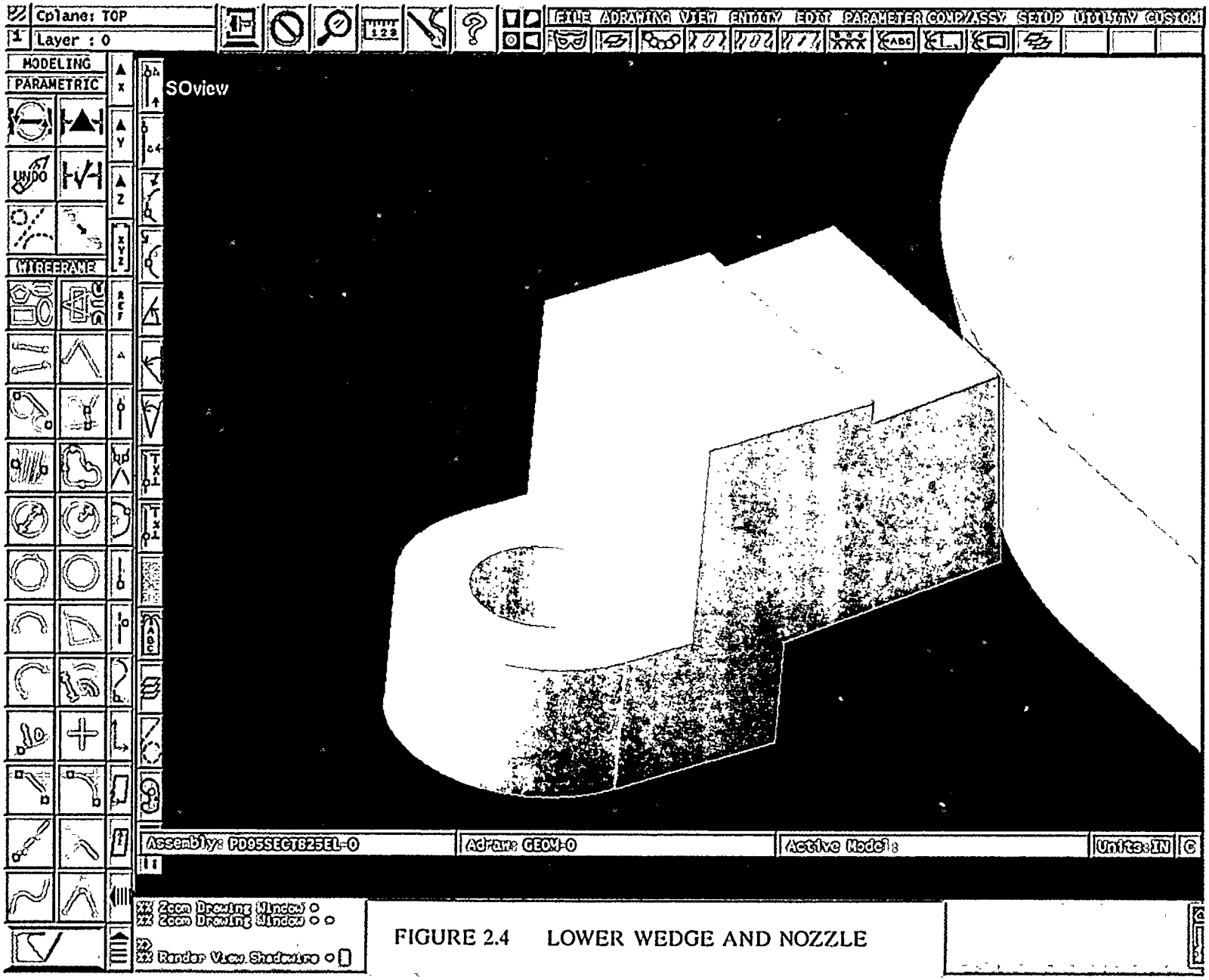

FIGURE 2.4 LOWER WEDGE AND NOZZLE

to maintain stability. The inspection video does not indicate a severe contact angle, but a precise contact angle cannot be determined.

Three dimensional computer drawn layouts were made of the nozzle region and the lower wedge. The layouts are based on the Combustion Engineering design drawings for the vessel and nozzle and the tie rod hardware drawings for the lower wedge. Since there are uncertainties between the design drawings and actual hardware, the attempt is to generate computer pictures looking like the inspection pictures. When the CAD layouts appear representative, the dimensional details can be quantified.

One of the inspection tapes showed a reverse angle perspective of the lower wedge which appears to indicate a different contact condition than was previously described. Figure 2.2 is a reverse angle view. Figures 2.3 and 2.4 are CAD pictures showing the lower wedge in contact with the blend radius. These figures show only a 3 inch thick slice of the vessel and nozzle to provide a contrasting background. Figure 2.3 is based on nominal layout dimensions and shows the lower wedge resting on a 2° to 3° incline surface. The incline is determined from alternate views made from the layout data base. This figure appears representative of the photo in Figure 2.2. Other views were generated with the contact located about 1 inch towards the nozzle opening, with the contact located 1.5 inches lower on the nozzle blend radius and with the contact located 1.5 inches lower and 1 inch towards the nozzle opening. The 1 inch and the 1.5 inches include the uncertainties in the layout dimension.

Figure 2.4 shows the contact located 1.5 inches lower than shown in Figure 2.3. There is little distinction between the computer pictures with the 1.5 inch vertical separation and both appear similar to the Figure 2.2 photo. The contact angle at the lower position may be somewhat higher (about 8°) than that based on the nominal dimensions. Neither of these figures can be used to conclusively identify the location of the lower wedge, but can establish a range for the contact angle. The layouts and the video provides assurance the lower wedge is not resting on a severe incline.

The view with the lower wedge moved 1.5 inces lower and 1 inch towards the nozzle rests on about a 22° incline nozzle does not appear representative. Both the vertical and horizontal angles do not appear as shown in Figure 2.2.

The location analysis and the additional concerns are summarized below. Additional analysis and evaluation address these items.

- Based on the inspection videos and a 3-D computer generated layout, the contact area is on the blend radius of the 258° nozzle and is most likely making contact on an inclined surface. The contact is over a smaller area than previously indicated.

- The original evaluation analyzed the lower spring as a rigid body. The offset load condition causes a twisting moment which changes the stress distribution in the lower spring and will change the loading on the tie rod components.

- The initial evaluation was presented as a conservative approach that relied on friction to balance the forces and moment in the free body diagram. The continued work in Sections 4.1 and 4.2 shows the assumed condition to be close to the actual configuration but the evaluation has to rely on friction as a condition of acceptability.

2.3 Contact Area

The contact area between the lower wedge and the nozzle radius is estimated from the available photos. Figure 2.2 shows the best view for estimating contact area. Using the 3.5 inch by 4 inch lower wedge dimensions as a reference for determining contact area, the contact area appears as a triangular surface 1.2 inches across the top and 2.1 inches down the side.. The resulting 1.26 $in.^2$ contact surface represents about 9% of the total 14 square inch contact surface. Because of the uncertainties in these dimensions, the calculated surface area is approximate. However, as seen later, the structural evaluations have been performed assuming point contact making the contact area not directly

relevant. The only aspect where contact area is important is in the bearing stress calculations. The vessel bearing stresses are low for normal operating conditions and are found acceptable for upset, emergency and faulted conditions. Potential yielding of the lower wedge will not affect the tie rod lower spring function.

2.4 Analysis Background

Field Deviation Disposition Request (FDDR) EA1-0032 documents the deviation of the tie rod lower wedge being in contact with the blend radius of the vessel recirculation outlet nozzle at 258°. Details of the discrepancy and evaluation were transmitted to the NRC March 23, 1995, in NMPC document NMP1L, *Generic Letter 94-03, "Intergranular Stress Corrosion Cracking of Core Shrouds in Boiling Water Reactors" (TAC No. M90102).*

The FDDR was evaluated and dispositioned as an acceptable condition. The evaluation considered the stability of the lower spring assembly, the hydraulic loadings on the lower spring, lower wedge bearing loads and the nozzle stresses. This evaluation was intended to be extremely conservative using the bounding load conditions. The disposition is summarized below.

- The lower spring was evaluated as a rigid body with the seismic load applied as a point load at the edge of the lower wedge. This offset load condition created a moment that was balanced by a friction load at the contact surface. The 0.12 friction coefficient required to maintain equilibrium was judged to be reasonable and acceptable for the stainless to stainless materials at the contact surfaces.

- The hydraulic pressure drop across the lower spring creates a transverse load which tends to peal the spring away from the C-spring. The bolt holding the lower spring to the C-spring was found capable of resisting this load condition.

- The lower wedge and vessel clad were also evaluated for bearing loads. The minimum contact area for normal operation preload bearing stress is only 1 percent of the available area and the bearing area required for seismic plus LOCA loads was determined to be only 10 percent. The contact area as described on the FDDR appeared more than sufficient to meet these requirements. The actual contact area was not a major concern for the FDDR evaluation. The 64k bearing load was used in this evaluation since it is the bounding load condition.

- The reaction on the nozzle was evaluated for the changes in the local stresses and for the overall stresses at the contact location. The stresses at the contact location were found to be acceptable since the stresses are less than the more highly stressed regions on the nozzle.

2.5 Operability Concerns

Each area of the original FDDR evaluation was addressed based on findings and concerns described above. The evaluation considered the stability of the lower spring assembly, the hydraulic loadings on the lower spring, lower wedge bearing loads and the nozzle stresses. All conditions are found acceptable. The tie rod assembly remains functional and will perform the design basis function of limiting the core support displacement.

The additional evaluations are summarized below.

2.5.1 Adequacy of Offset Wedge Contact Seating on the Nozzle

The FDDI analyzed the lower spring as a rigid body with the seismic load applied at the edge of the contact. Friction was considered to balance the moments resulting from the offset load.

Computer generated 3-D layouts of the nozzle and lower contact show the point of contact on the blend radius of the 258° outlet nozzle. The contact angle at the point of contact appears to be 2° to 8°. The 8°

contact location takes into account the uncertainties in the layout dimensions. Assuming a 0.2 friction coefficient, the contact will be stable (not slip) until the contact angle reaches 11.3°. As shown in Section 4.2, the tie rod stresses are acceptable even with contact angles up to 22°.

Additional work was done to analyze the lower spring as an elastic body to determine the maximum stresses and the stress distribution that results from the offset load condition. The offset loading also produces a twisting in the lower spring which affects the loads on the pin connecting the lower spring to the C-spring. If the lower wedge does not slip, the pin does not react against the seismic load but only to the twisting that occurs at the pin location. The loads and resulting stresses are limited by the degree of twist at the pin location.

The lower spring, by design, does not rely on the connecting pin to carry any load other than to support its own weight. The connecting pin is not in the load path for the seismic loads. The pin is loaded only by the elastic distortion of the hole in the lower spring and those loads and stresses have been calculated and found acceptable.

The worst case for spring twisting is as shown in the original load diagram included in the NMPC March 23, 1995 letter. The detailed analysis for this load condition (Appendix I) show all stresses remain below the allowable stresses.

Other load conditions were also considered for the lower spring. The lower spring loads were evaluated in Section 4.1 for the spring bearing on an inclined surface where friction is sufficient to maintain stability. The tie rod assembly was also analyzed in Section 4.2 for upset, emergency and faulted load conditions with the contact resting on a 22° incline where slipping is considered. In both cases the shroud repair hardware stresses are acceptable.

2.5.2 LOCA Transverse Loads on Spring

The original evaluation included in the NMPC March 23, 1996, letter considered a hydraulic prying load on the lower spring that may occur during an emergency and faulted LOCA event. The prying load is resisted by the pin connecting the lower spring to the C-spring.

During a recirculation line LOCA, the lower spring may have an estimated 40 psid on the projected area in the flow field. This pressure results in a 7.2 kip load tending to pry the lower spring away from the C-spring. The analysis shows the pin is capable of resisting this prying moment.

The spring twisting caused by the assumed offset load conditions during a faulted seismic event also adds loads to the pin. This combination was not previously evaluated.

During a seismic event, the spring is compressed between the shroud and the contact on the nozzle blend radius. The friction at the contact make the spring act like a simply supported beam rather than a cantilever as was assumed in the original analysis. The 7.2k hydraulic load is assumed equally distributed between the connecting bolt and the spring loaded contact surfaces. The bolt stress for this condition is 7.2k/(2 x 0.97 sq. in.) = 3.7ksi. This stress when added to the pin stress due to twisting (Appendix I) remains below the bolt allowable stress.

The friction coefficient required to support the lower spring in the assumed simply supported beam configuration is the required azimuthal load divided by the normal spring load. Required friction coefficient =3.6/64 = 0.06. The total friction required to balance the offset load (0.12 from NMPC March 23,1995 letter) and to resist the hydraulic load (0.06) is 0.18. This remains below the 0.2 friction coefficient assumed for the stainless to stainless material couple.

The pin twisting stresses under seismic loading combined with the hydraulic load stresses remain acceptable.

2.5.3 Wedge Bearing Contact Adequacy

The inspection video and the layouts indicate the lower contact with only partial engagement with the nozzle blend radius. The inspection video show a triangular contact surface with about 1.2 inch engagement along the top surface and 2.1 inches along the vertical edge. The expected 6000 lb load for normal operating conditions are easily satisfied with the reduced contact area. A finite element analysis using a 1 inch square contact area show the vessel bearing stresses are acceptable with the high loads experienced during a upset and faulted seismic events. Appendix II contains the details of the vessel bearing stress analysis. The stresses in Type 316 stainless steel lower wedge exceed the 1.5Sy bearing stress allowable for an. upset seismic event in the region of the contact. Yielding can occur at the lower wedge contact surface during this short duration load condition, but this will not affect the function of the lower spring. Thus, the reduced contact area will not affect the ability of the lower spring to limit the core plate displacement.

Bearing loads applied near a free edge must also be evaluated for shear. The shear plane is along the diagonal edge of the triangular contact surface. The 8 inch thick shear plane includes the thickness of the added foot, the lower wedge and the spring. All these items are in intimate contact and failure can only occur if all members fail. For an upset event, the allowable shear stress is 0.6 Sm or 10,500 psi for the 316 sst foot and lower wedge. The required length of the diagonal edge of the contact area is less than 0.76 inch to satisfy this requirement. The actual length of the diagonal is greater than 2 inches which provides adequate margin.

2.5.4 Stress Impact of the Lower Spring on the Nozzle Blend Radius

The analysis includes the evaluation of the lower contact bearing on the nozzle blend radius . The effect of a contact load on the nozzle blend radius has been evaluated and is reported in Appendix II. The calculated contact stresses are combined with the maximum nozzle stresses as reported in the original Combustion Engineering analysis. The combined stresses are compared against the allowable primary stresses and are found acceptable.

During a seismic event the spring 180° from the load bearing spring may lose contact with the RPV (or nozzle blend radius). The resulting impact loads, which develop when the gap closes and the opposite spring re-engages with the vessel wall, have been evaluated and found to be bounded by the loading during a seismic event. The maximum impact load magnitude is less than one-fifth of the maximum spring compression load experienced during a seismic event and is acceptable.

Furthermore, the maximum value of the impact load occurs at the maximum relative velocity and zero spring compression. The maximum spring compression occurs at zero relative velocity. Consequently, the maximum value of impact load and the maximum seismic spring compression loads are not additive. The spring compression load is the bounding load.

2.6 Effect of Thermal and Seismic Displacement

Both the RPV and the tie rod assembly experience thermal growth during reactor heatup. Significant differential movement between the lower wedge and the RPV could affect the contact location as seen in the inspection videos.

The expansion coefficient of the vessel material (7.125×10^{-6}) and the Inconel lower spring (7.5×10^{-6}) are similar and the relative movement between the lower wedge and RPV is small. With both the tie rod assembly and RPV at

550°F, the net axial movement between the lower wedge and RPV is about 0.01 inches.

During a thermal transient, the tie rod assembly is assumed to rapidly cool to 300°F while the thermal mass of the RPV maintains its temperature at 550°F. Under these conditions the net relative axial movement between the lower contact and vessel is about 0.09 inches. These small movements have insignificant effect on the stability evaluation for the lower wedge.

During a seismic event, the lower springs may lose contact with the RPV and become free to move laterally. This movement is limited by the clearances in the connecting parts. The lower spring is firmly attached to the C-spring and the C-spring is restrained by the lower support. The maximum clearance at the C-spring and lower support interface is 0.12 inches. This is the maximum lateral movement the lower spring can experience. The axial tension in the tie rod tends to prevent any lateral movement. The 0.12 inch possible movement is not significant for evaluating the lower wedge stability.

3. APPLIED LOADING

The lower spring has a nominal preload forcing the lower wedge on the vessel surface. The radial force is small and is intended only to assure contact with the vessel. Therefore, the applied loading on the lower spring during normal operation is negligible and has no impact on the spring. The only time that the spring experiences a significant load is during a seismic event. If the spring was in contact with the vessel surface, the seismic force would be reacted radially and there is no twisting moment on the lower spring. However, for the 270º tie rod assembly, the radial force is applied at the edge of the lower wedge and possibly on an inclined surface. Figure 3-1 shows a schematic of the loading for point contact, but on an inclined surface at an angle. The seismic loading F_s is radial and would be reacted by a normal force if the contact were on the vessel surface instead of the nozzle. With the contact at an angle α, the seismic load produces a normal force $F_s \cos \alpha$ and a tangential force $F_s \sin \alpha$. The tangential force is resisted by the friction force $F_f = \mu F_{normal} = \mu F_s \cos \alpha$ where μ is the friction factor. As long as the friction force exceeds the tangential force, there will be no slipping. The angle for which the friction force is just equal to the tangential force is given by:

$$F_s \sin \alpha. = \mu F_s \cos \alpha, \text{ or, } \tan \alpha. = \mu.$$

If a conservative friction factor of 0.2 (see Appendix IV for justification) is assumed, the angle at which slipping could occur is given by $\tan \alpha. = \mu.=0.2$ or , the angle for slipping is 11. 3 degrees. For the purposes of analysis two loading conditions were considered. The first case assumed that there was no slipping (expected even with the worst case angle of contact and assuming a friction factor of 0.2). The second case ***postulated*** a contact angle of 22º and considered the stresses in the hardware for this bounding condition:

a. The seismic load is applied to the outer edge of the contact. This condition results in the most severe twisting moment on the lower spring. If the spring is assumed to bear against an inclined surface, the moment caused by the side load at the inclined surface acts in the opposite direction to the moment caused by the edge load.

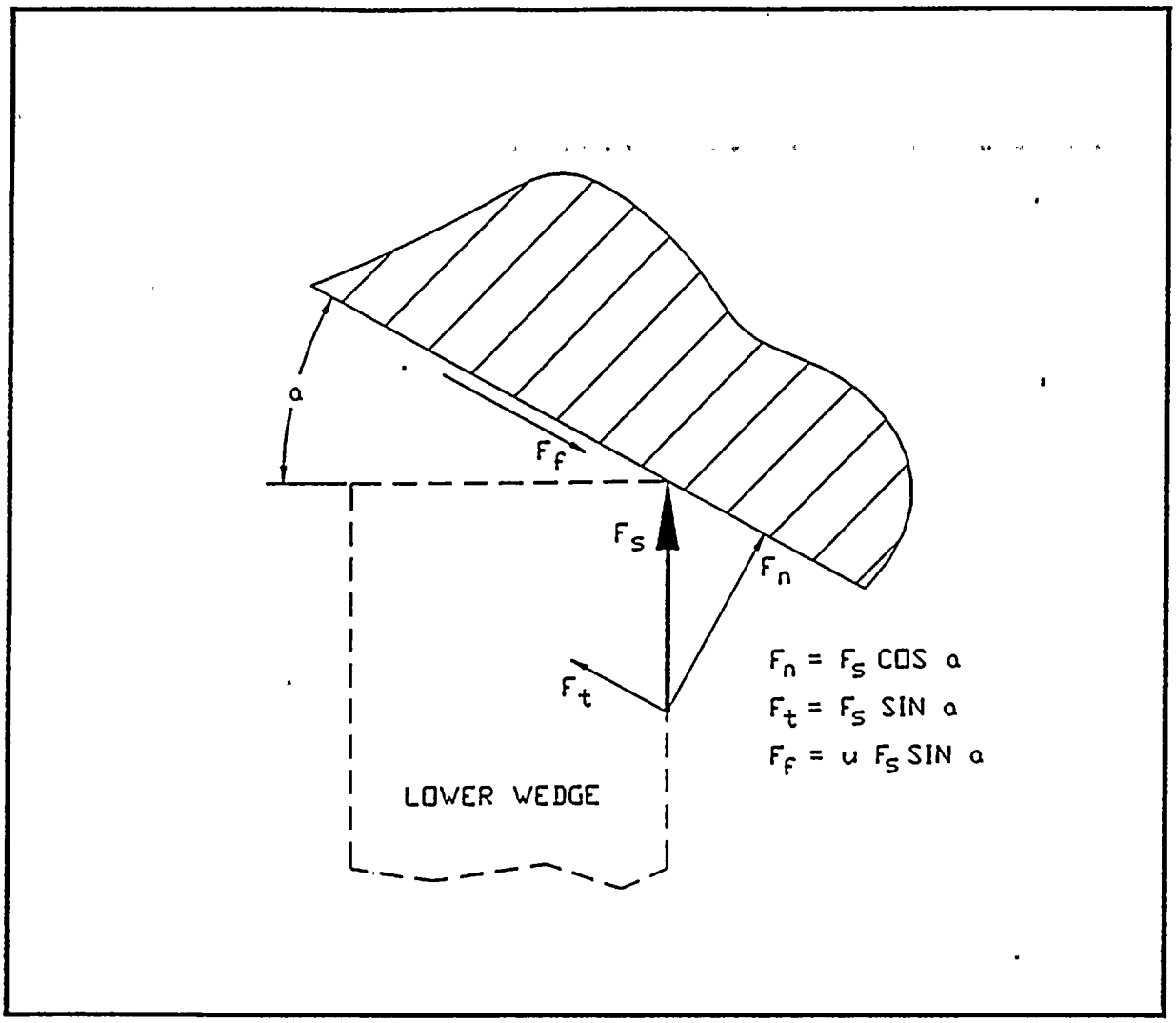

Figure 3.1
Load Schematic

b. The lower wedge was *assumed* to bear against a 22° inclined surface where the assumed friction is not sufficient to prevent slipping. The resulting side load increases the stresses on the pin connecting the lower spring to the tie rod assembly and to the other tie rod assembly component. Appendix I shows the applied loads for this condition.

As discussed in Section 4, the stresses in both cases were acceptable.

4. STRUCTURAL ANALYSIS AND SAFETY ASSESSMENT

The structural analysis and safety assessment of the 270º tie rod assembly in the as-installed condition is described in this section. The structural assessment considers a series of increasingly conservative postulates on the condition of the 270º tie rod assembly. First (in Section 4.1) it is assumed that there is point contact of one edge of the wedge on the nozzle (but no slipping), resulting in a twisting moment on the lower spring and it is shown that the stresses in the hardware are within the specified limits. In section 4.2, point contact is assumed as before, but slipping is also allowed. This applies a lateral load on the lower spring that tends to bend the pin connecting the tie rod to the lower spring. As described in Section 2, it is estimated that the contact angle could range from 2º to 8º depending on the tolerances. In order to account for potential uncertainties in the 8º estimate, it was assumed conservatively that the contact point is one inch away from the expected location. This corresponds to a contact on a slope of 22º into the nozzle. It is shown that even with contact occurring on a 22º slope surface, the lateral force will not lead to failure of the pin. In Section 4.3, it is assumed that the lower spring is totally ineffective (no resistance to lateral motion of the shroud) and it is shown that even in this condition, the lateral displacements are not high enough to impede control rod insertion.

4.1 Analysis Assuming Point Contact, but no Slipping

A structural analysis (Appendix I) of the tie-rod stabilizer assembly was performed for this case assuming a point contact radial loading on the lower spring with no circumferential sliding. The load is applied at the outer edge of the lower wedge. This loading results in the highest twisting moment on the lower spring. The analysis was performed by developing a Finite Element Model (FEM) and analyzing the stresses of the lower spring, C-spring, tie rod and connecting pin. Figure 4.1 shows the FEM model of the lower spring and the C-spring. The overall model also includes, but not shown in Figure 4.1, the tie rod, the clevis pin and the pin connecting the lower spring to the C-spring. These items were modeled as 3-D beam element.

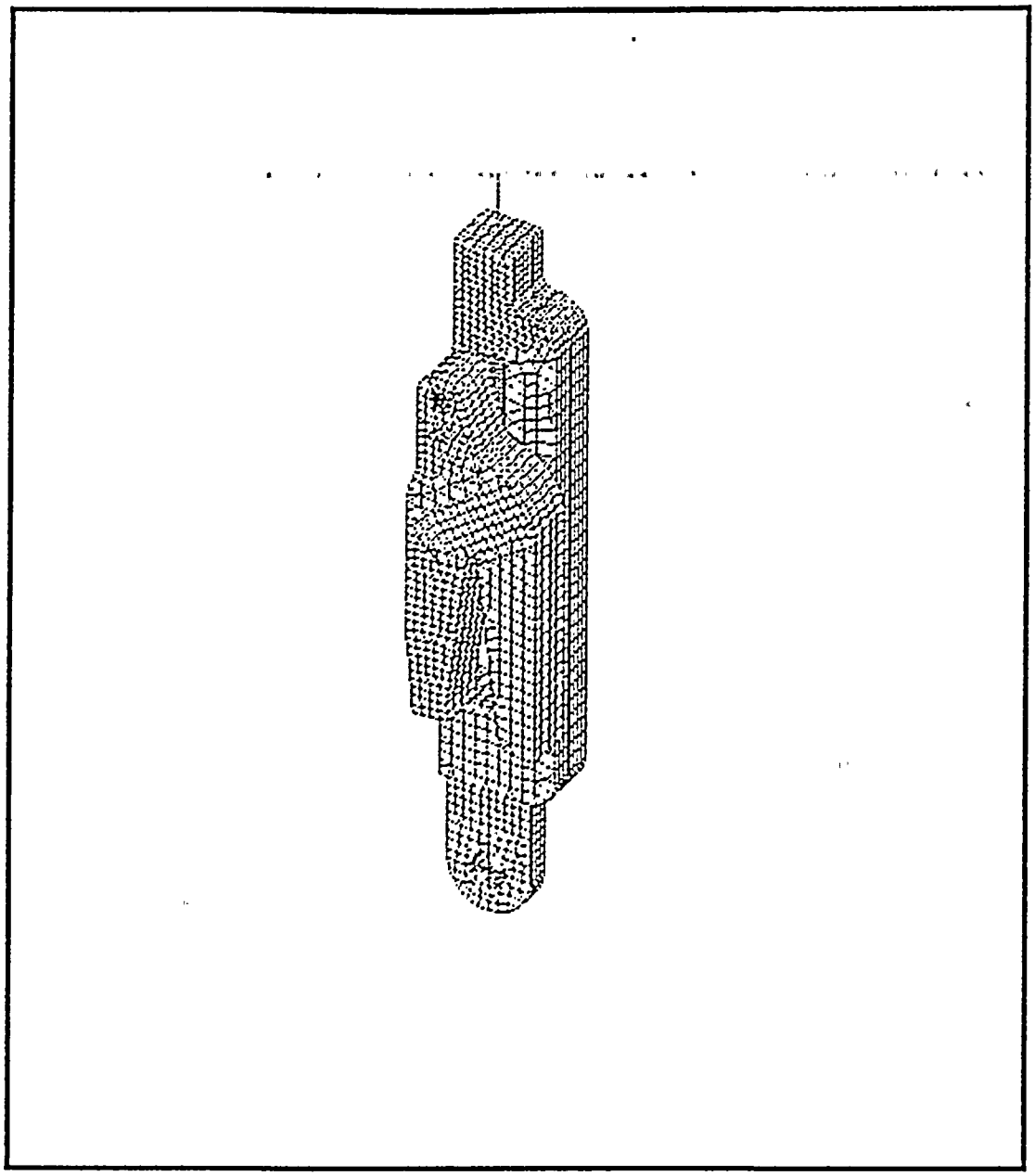

Figure 4.1
Lower Spring and C-Spring Finite Element Model

The analysis was performed for Normal, Upset, Emergency and Faulted events. The load cases included the limiting axial and seismic loads for each event. The maximum calculated stresses in the lower spring, the C-Spring and the tie rod are only slightly higher than reported in the original stress report and all well below the allowable stress limits. The pin connecting the lower spring to the C-spring was not previously evaluated since its only function is to support the weight of the lower spring. The twisting moment applied to the lower spring may also put a load on the connecting pin. The analysis show this load to be small and the pin stresses are well below the allowable stress limits. The results showed that all the component stresses were acceptable and met the allowable limits.

It is therefore concluded that under the assumptions stated above, the structural integrity of the tie-rod stabilizer assembly is maintained for the postulated seismic event. Hence, the safety function of the tie rod assembly is not adversely affected.

A similar stress analysis was performed for the nozzle blend radius of the Reactor Pressure Vessel (RPV), which is included in Appendix II. Basically, the stresses at the recirculation outlet nozzle which were obtained from the previous RPV stress report (due to pressure) were conservatively combined with the stresses due to point contact seismic loading from the RPV code stress report. The results show that the recirculation outlet nozzle stresses are acceptable and meet the ASME pressure boundary stress limits. It is therefore concluded there is no adverse effect on the safety function of the RPV during the postulated seismic event.

4.2 Analysis Assuming Point Contact and Slipping

The lower spring was analyzed for point contact and possible slipping along the inclined contact surface. The lower spring was evaluated for this condition at maximum spring compression during a seismic event. This case was addressed as an addendum to Appendix I stress analysis. For this purpose, a hypothetical circumferential point load was applied to the lower spring in addition its radial seismic load and the tie rod axial load. The circumferential load was calculated

for the lower wedge bearing against a slope of 22°. This 22° angle is greater than the 11.3° critical angle associated with a 0.2 friction coefficient and the wedge will tend to slide. The forces available to resist sliding are provided by the pin connecting the lower spring to the C-spring and by friction at the contact surfaces. For a 22° contact surface, the unbalanced circumferential load at the inclined surface is 12,107 pounds. A circumferential friction force of 12,760 lb. is available at the shroud contact surface to help resist the slipping. The pin must provide the remainder of the force to prevent slipping.

This 12,107 pound load applied to the lower spring in the circumferential direction tends to pry the lower spring from the C-spring. A large part of this load is reacted by the friction at the shroud contact. The pin sees only a small portion of the prying load. The pin connecting the lower spring to the C-spring was evaluated for two conditions. The first case the prying load is resisted by the pin in bending. The analysis show the pin bending stresses remain below allowable stress limits for upset events and for steam line LOCA plus seismic emergency and faulted events.

The second case assumes the prying effect is resisted by the lower spring contacting the C-spring. In this case the pin is loaded in tension. The analysis show the pin primary tensile stresses remain below allowable for the upset events and for steam line LOCA plus seismic emergency and faulted events.

The analysis shows that the pin is able to prevent the lower wedge from slipping at contact angles of up to 22° without overstressing the connecting pin. At contact angles greater than 22° slipping may also occur at the shroud contact which significantly increases the load on the pin. At about 23.5°, the pin stresses will exceed the ASME Code allowable stresses. At 22°, no migration of the spring down the nozzle is expected to occur. Thus, even in this load case, the safety feature of the tie-rod stabilizer system is not compromised.

4.3 Analysis Assuming that the Lower Spring is Ineffective

4.3.1 Introduction

In the previous sections, the acceptability of the 270º lower spring was evaluated assuming offset loading, with and without sliding. In this section, the postulated case of the 270º lower spring being completely ineffective (i.e., no lateral resistance) is evaluated. The case of one lower spring (270º stabilizer) being ineffective, but the remaining springs being intact is difficult to analyze for seismic loading since the seismic model is a linear cantilever beam element model with a single lateral spring simulating the combined effect of all four lower springs. Thus with the seismic model it is possible to analyze only the two extreme cases: all lower springs intact or all lower springs being ineffective (i.e., no lower spring). A reasonable assumption is that the displacements for the case of the 270º spring alone being ineffective is bounded by the two extreme cases, with and without the lower spring in the seismic model. The following discussion considers the case of no lower springs and shows that for this extreme case, the ability to scram is still maintained. Since the lower spring intact case has already been addressed in the original analysis, the two extreme conditions together assure that the specific case of the 270º spring being ineffective is also addressed.

In support of the 270° tie rod assembly evaluation, additional seismic analysis cases were run assuming the lower spring to be ineffective. Two governing conditions were analyzed: with no separation (all hinged case) and with separation (H6b on rollers and other welds hinged). The first condition addresses seismic + normal operation or seismic + recirculation break while the second condition considers seismic + steam line break. The results of the two evaluations are described here.

<u>DBE + recirculation break (All hinged model)</u>

To evaluate the all hinged case without the lower springs, a more realistic seismic model that accounts for the rotational stiffness of the shroud at the hinge as a result of tie rod elongation and considers the restoring moment due to the weight of the shroud was used. The details of the new seismic modeling approach are described in Appendix III.

The new model has been used for shroud repair in other plants and has been reviewed with the NRC for one plant unique submittal (Appendix III). This analysis procedure more closely simulates the true shroud behavior, especially in an "all welds cracked" case. The procedure accounts for the cylindrical shroud geometry and incorporates the restoring moment offered by the dead weight of the shroud above the crack plane. This method mitigates the displacements predicted when assuming a simple idealized hinged beam. The Nine Mile 1 shroud has been analyzed by this procedure assuming all welds cracked and without the lower spring. The seismic + recirculation line break displacement at the core plate, without the lower spring, is calculated to be 0.03 inches. This assures that for a seismic event accompanied by a recirculation line break, the displacements are small and well within the allowable values in the design specification. Therefore the ability to scram is assured for this faulted event.

DBE + steam line break (Rollers at H6b)

This case simulates the combination of steam line break coupled with a seismic event and is bounded by the case of rollers at H6b and hinges at all other locations. The pressures during a steam line break are sufficient to cause separation for approximately two seconds, after which the weight of the shroud is sufficient to assure contact at all welds. In order to simulate this, the maximum displacement for the steam line break during the first two seconds was calculated using the roller model, but subsequent motion would be represented by the all hinged case previously described. The maximum displacement during the first two seconds using the roller model was determined to be 0.58 in. This is well below the allowable reversing elastic displacement limit of 1.5 inch (from the design specification). Even if one assumes that this is a permanent displacement (instead of a reversing motion) it is below the limit of 0.67 inch limit in the design specification for the faulted condition. Control rod insertion is assured without any negative effect on scram time for displacements below this limit.. Subsequent displacements under the

hinged condition are small, thus assuring that the ability to scram is maintained.

5. OTHER SAFETY CONSIDERATIONS

5.1 Flow Induced Vibration

Flow Induced Vibration (FIV) of the tie rod assemblies was evaluated in the original modification stress report. The tie rods are threaded at both ends and are 3.5 inches in diameter and 136.6 inches long. The top end is connected with a nut to support the assembly while the bottom end is threaded into the axial C-spring member. The C-spring member is, in turn, anchored to the core shroud support cone by a pin and clevis arrangement. The tie rod assembly is mechanically preloaded to 3,000 lbs and thermally preloaded to 79,600 lbs for a total preload of 82,600 lbs.

The maximum value of the vortex shedding frequencies due to the reactor coolant flow along the length of the tie rod assemblies was determined in to be 7 Hz. This value is independent of whether or not the lower stabilizer spring bearing surface contacts the vessel inner wall.

As reported in the original modification stress report, a Finite Element Model (FEM) of the tie rod assembly was developed to help assess the effect of the FIVs. The tie rod assembly FEM was comprised of 3-D beam elements and was constrained at: (i) the upper bracket attachment to the shroud, and (ii) the pin/clevis location on the C-spring (iii) the upper spring contact points on the vessel, (iv) the mid-support spring contact point on the vessel, (v) the lower spring contact points on both the vessel and the shroud. In general, all translation and rotational degrees-of-freedom (DOF) were constrained at these locations except the rotational DOF in the tangential direction at the pin/clevis location at the bottom of the C-spring.

Because of the boundary conditions assumed at the spring contact surfaces, the shroud lower stabilizer springs contribute to the lateral stiffness of the tie rod assembly and therefore to the magnitude of its fundamental frequency. The calculated tie rod assembly fundamental frequency was 28.16 Hz. When the lateral stiffness contribution due the lower spring was removed from the tie rod

assembly FEM, the lower bound fundamental frequency of the assembly was calculated to be 15.2 Hz. This latter calculation corresponds to the condition of the lower spring becoming ineffective as the spring contact surface, for the spring located at the 270° azimuth, migrates a sufficient distance onto the vessel inner wall flared surface associated with the vessel penetration. Both calculations accounted for *only the flexural stiffness* of the beam elements which comprised the tie rod assembly and the assumed boundary conditions. They *did not account for the mechanical and thermal preloads.* Consequently, these lower bound values are very conservative and the actual values are significantly higher.

The total magnitude of the mechanical plus thermal preload in the tie rod assemblies which was not included in the foregoing fundamental frequency calculations is equal to 82,670 lbs. A second calculation for the lower bound fundamental frequency of the tie rod assembly, based on the magnitude of the tie rod preload and *neglecting the tie rod flexural stiffness,* yielded a value of 14.0 Hz.

Denote the tie rod assembly fundamental frequency based only on the flexural stiffness of the tie rod elements by ω_1 (where ω_1 = 15.2 Hz) and that based only on the tie rod preload by ω_2 (where ω_2 = 14.0 Hz). Then

$$\omega_1 = [k_1 / m]^{1/2} \rightarrow k_1 = m\,\omega_1^2 \qquad .....(1)$$

and

$$\omega_2 = [k_2 / m]^{1/2} \rightarrow k_2 = m\,\omega_2^2 \qquad .....(2)$$

The equivalent stiffness which accounts for both the flexural stiffness and the preload in the tie rod assembly is denoted by k_e and is given by

$$k_e = k_1 + k_2 = m\,[\omega_1^2 + \omega_2^2] = m\,\omega_e^2 .....(3)$$

where the equivalent frequency is denoted by ω_e. Therefore

$$\omega_c = [\omega_1^2 + \omega_2^2]^{1/2}$$
$$= [15.2^2 + 14.0^2]^{1/2} = 20.7 \text{ Hz} \qquad \text{.....(4)}$$

Equation (4) corresponds to a lower bound of the fundamental frequency of the tie rod assembly when both tie rod flexure and tie rod preload are accounted for in the calculation. Therefore, the FIV vortex shedding frequency of 7.0 Hz is less than one-third of the tie rod assembly lateral fundamental frequency. Consequently, the tie rod assembly is essentially rigid (at the least quasi-rigid) with respect to the frequency content of the FIV excitation and the FIVs are therefore insignificant.

5.2 Core Shroud Cracking Probability Review

This section discusses the potential for shroud cracking exceeding the minimum structural ligament requirements. This will be used to provide the reasoning for the conclusion that cracking is not expected to the extent that minimum structural requirements will be exceeded.

5.2.1 Minimum Structural Ligament Requirements

The determination of the minimum structural requirements has been previously performed. The evaluation of allowable flaw sizes includes significant conservatism which provides confidence in the safety margins. Two methods have been used to determine the allowable flaw sizes for the shroud welds. The first involves determination of the allowable through-wall single flaw. This method conservatively combines the indications in the worst orientation with respect to the applied loading. The second and more realistic method is the flaw evaluation approach which takes into consideration the location of the indications in determining if the safety factors are met for the given flaw distributions. Both of these methods conservatively assume that the flaws are through-wall.

In the flaw evaluation approach, the through-thickness depths can also be accounted for if available. Including even small remaining ligaments into the calculations results in significant increases in safety margins. This has been verified by using actual results from UT inspections. In cases where fully circumferential flaws are considered, it has been shown that very little remaining ligament is required to satisfy structural requirements. Calculations have shown that typically, the required remaining ligament can be as little as 5% of the shroud wall thickness.

5.2.2 Field Experience

Inspection of core shrouds has been performed at almost every GE BWR in the world. Only three core shrouds have not been inspected. In addition, inspection of several non-GE BWR's has also been performed. Many of these inspections have been performed using sophisticated volumetric inspection techniques resulting in detailed position and depth characterization of the indications. There has never been a case of 360° through-wall cracking in the core shroud. It should be noted that in NUREG-1544, the NRC staff noted that, i) no 360° through-wall core shroud cracking has been observed to date in any US BWR at which the licensee performed a shroud inspection, and ii) no US BWR has exhibited any of the symptoms (power-to-flow mismatch) that would be indicative of leakage through a 360° through-wall shroud crack.

Extent of cracking has ranged significantly based on these inspection results. Generally, cracking has been more extensive for those plants which have operated longer and those which have had poorer water conductivity. In addition, significant cracking has been observed in machined rings (core plate and top guide support rings). Significant cracking in these rings was possibly caused by elongated inclusions or stringers because of exposure of surfaces oriented in the short transverse direction.

For those plants which have UT inspection results available, indication depths have ranged significantly. For some plants with plate rings, continued operation has been justified based on allowable flaw calculations which have demonstrated that the fillet weld provides sufficient structural reinforcement. Typically, maximum crack depths have been found to be on the order of 0.75 inch, significantly below the allowable 360 degrees flaw depth.

The crack depth usually varies significantly around the shroud circumference. UT results from several plants with significant circumferential cracking show some "spikes" (local areas of deeper cracking) superimposed on an average crack depth. In general, average crack depths are significantly lower than the spikes. For an example plant, the peak depths were 0.75" compared to an average depth of approximately 0.4".

5.2.3 Potential For Through-Wall Cracking

As discussed in Section 5.1.3, there have not been any cases of through-wall cracking in a core shroud such that leakage has occurred. The propagation of a crack through a relatively thick section such as the shroud is dependent on several conditions. These include a driving force for crack propagation and the existence of an aggressive environment.

The weld residual stress at the welded shroud locations is the main driving force for IGSCC growth. The weld residual stress distribution in the shroud wall is likely similar to that for a double sided weld in a thick flat plate. The stress is tensile on the inside and outside surfaces and is compressive in the center portion of the wall. With crack propagation, the weld residual stress tends to relieve itself, and the overall magnitudes of the distribution reduce.

Water chemistry, primarily water conductivity, has improved at NMP1 since initial startup of the plant. The improved water chemistry record at NMP1 will have a significant impact on crack growth rates of existing indications. UT inspections performed at several plants can be used to determine more realistic crack growth rates. Typical current analyses of shroud cracking use a crack growth rate of $5x10^{-5}$ in/hr. This value has been found to be very conservative compared to the values based on field experience. By comparing crack depths and lengths from subsequent UT inspections, a more realistic crack growth rate in the depth direction is $2.5x10^{-5}$ in/hr. The fact that cracks have not grown through-wall after many years of operation, which using the $5x10^{-5}$ in/hr rate would suggest, suggests that indeed the crack driving force and improved water chemistry has resulted in much smaller crack growth rates and possible arrest of the indications.

In addition to the reduction in weld residual stress, the application of the shroud repair will result in a compressive membrane load on the core shroud circumferential welds. These compressive membrane stresses would add to the reduction of driving force for further crack propagation.

With the consideration of significant reduction of weld residual stress with crack growth, improved water chemistry conditions, it is considered highly unlikely that on a 360° basis, the crack growth would grow beyond the allowable flaw depth. Again, this conclusion is supported by the absence of through-wall cracking in any core shroud.

6. CONCLUSIONS

Following the installation of the core shroud repair at Nine Mile Point 1 (NMP1), a visual inspection of the as-installed hardware showed that the lower spring wedge of the 270º tie rod assembly was bearing against a recirculation nozzle weld instead of the vessel. As a result of the slope on the nozzle surface, the contact area was approximately 2/3 of the full wedge area. Since then additional review of the videotapes and 3D Computer Aided Drafting (CAD) layouts have shown that the actual wedge contact area is less than the originally estimated 2/3 and may be as low as 9% of the full wedge area. Also, the wedge contact is on an inclined surface of the nozzle. A technical evaluation of the adequacy of the 'as-installed' condition of the 270º tie rod assembly was performed so that the effectiveness of the repair could be confirmed.

Worst case assumptions of the as-installed condition (based on dimensional tolerance limits) were reviewed and the related operability concerns were evaluated. In particular, limiting conditions on the contact area (point contact assumed) and wedge contact angle (slipping with 22º angle, based on uncertainty of one inch on the expected location of the wedge) were considered. The structural analysis and safety assessment considered a series of increasingly conservative postulates on the condition of the 270º tie rod assembly - point contact of one edge of the wedge on the nozzle (but no slipping), point contact with a 22º angle with slipping and finally assuming that the lower spring is totally ineffective. In all cases control rod insertion and safe shutdown are assured. Other safety considerations such as the potential for flow induced vibrations (FIV) and the probability of additional shroud cracking were evaluated and found to be acceptable.

The evaluations performed have bounded the installation uncertainty associated with the 270° tie rod lower spring location. These evaluations have demonstrated that the horizontal support safety function provided by the tie rod lower spring assembly are assured given a location shifted 1 inch toward the nozzle centerline. The 1 inch uncertainty is judged to be consistent with an upper bound uncertainty for location. The analyses have also demonstrated that the tie rod axial support function is

maintained and is adequate to limit the maximum core plate displacement to within allowable limits even if the lower spring fails to function.

Based on the evaluations described here, it is concluded that the as-installed condition of the 270º tie rod assembly is acceptable and that all safety functions provided by the shroud repair are maintained.

7. APPENDICES

Appendix I: Detailed Stress Analysis of the Hardware with Offset Loading and Considering Slipping

Appendix II: Effect on Vessel Stress Analysis

Appendix III: Description of the Improved Seismic Model

Appendix IV: Friction Factor Documentation

APPENDIX I

Detailed Stress Analysis of the Hardware with Offset Loading and Considering Slipping

APPENDIX II

Effect on Vessel Stress Analysis

GE Nuclear Energy

24A6426	SH NO. 1
REV. 3	

REVISION STATUS SHEET

DOC TITLE REACTOR PRESSURE VESSEL

LEGEND OR DESCRIPTION OF GROUPS

| DENOTES CHANGE

TYPE: STRESS REPORT

FMF: NINE MILE POINT 1

MPL NO: PRODUCT SUMMARY SEC. 7

THIS ITEM IS OR CONTAINS A SAFETY RELATED ITEM YES X NO ☐ EQUIP CLASS CODE P

REVISION			C
A	RM-01715 17 NOV 1994		
1	J. TROVATO 19 DEC 1994	RJA	
	CONTROL ISSUE RM-01502 CHK BY: J. TROVATO		
2	J. TROVATO 10 / 04 / 95	RJA	
	CATEGORY III CHANGE CORRECTED ERM CALLOUT FOR REV 1 FROM RM-01502 TO RM-01840.		
3	J. L. TROVATO MAR 2 5 1996	RJA	
	CN03781 CHK BY: J. L. TROVATO		

PRINTS TO

MADE BY	APPROVALS	GENERAL ELECTRIC COMPANY 175 CURTNER AVENUE SAN JOSE CALIFORNIA 95125
J.L. TROVATO 17 NOV 94	B.N. SRIDHAR 17 NOV 94	
CHK BY	PRODUCT DEFINITION	
J.L. TROVATO 17 NOV 94	R.J. AHMANN 17 NOV 94	CONT ON SHEET 2

1. SCOPE

1.1 This document is the ASME Code Section I Paragraph N-142 Stress Report for the Reactor Pressure Vessel. This analysis addresses the new loads applied to the vessel as a result of the installation of the shroud stabilizers, which function to replace the horizontal girth welds H1 through H7 in the core shroud.

2. APPLICABLE DOCUMENTS

2.1 General Electric Documents. The following documents form a part of this stress report to the extent specified herein.

2.1.1 Supporting Documents

a. Code Design Specification 25A5586 Rev 1

b. Shroud Repair Hardware Design Specification 25A5583 Rev 1

2.1.2 Supplemental Documents. Documents under the following identities are to be used with this stress report.

None

2.2 Codes and Standards. The following documents of the specified issue form a part of this specification to the extent specified herein.

2.2.1 American Society of Mechanical Engineers (ASME) Boiler and Pressure Vessel Code

a. Section I, 1959 Edition and Addenda through Summer 1963 including code cases 1270N, 1272N, 1273N, 1275N.

2.2.2 Other Documents

a. General Electric Drawing 237E433 P1, Sht. 1, Rev. 9.

b. General Electric Drawing 237E434, Sht. 1, Rev. 5, "Reactor Thermal Cycles".

c. Combustion Engineering Report, October 1970, "Analytical Report for Niagara Mohawk Reactor Vessel" (VPF #1236-153-1).

d. GENE-B13-01739-04, Rev. 1, Shroud Repair Hardware Stress Analysis

3. GENERAL DESCRIPTION

3.1 The purpose of the shroud stabilizers is to structurally replace all of the horizontal girth welds in the core shroud. These welds were required to both horizontally and vertically support the core top guide, core support plate, and shroud head, and to prevent core bypass flow to the downcomer region. The core top guide and core support plate horizontally support the fuel assemblies and maintain the correct fuel channel spacing to permit control rod insertion.

3.2 The design requirements for the shroud stabilizers were separated into two documents. The first document addressed those requirements that were not under the jurisdiction of the ASME Code (Paragraph 2.1.1.b). The second document addressed those requirements that were under the jurisdiction of the ASME Code (Paragraph 2.1.1.a).

3.3 This Stress Report documents the acceptability of the structural integrity requirements of the Code Design Specification defined in Paragraph 2.1.1.a.

4. ANALYSIS

4.1 The Design Specification (2.1.1.a) defines five new design mechanical loads on the reactor pressure vessel. These loads F1, F2, F3, F4 & F5 and their point of application are shown in Figure 1 and Table 1. Each of F1, F2, F3, F4 and F5 is addressed below.

4.2 The force F1 is applied to the reactor pressure vessel (RPV) shell 380.18 inches above the RPV 00 elevation. It is a local force applied in the radial direction by the shroud repair during a Design Basis earthquake (DBE). At this elevation the RPV shell is 7.125 inches thick minimum (2.2.2.c).

4.2.1 A finite element (FE) model of a cylindrical shell of thickness 7.125" was developed and a radial load of 21.63 kips was applied. The model and the results are shown in Figures 2, 3, & 4.

4.2.2 The maximum value of Pl stress intensity due to this load is 0.09 ksi and the maximum value of Pl + Pb stress intensity is 0.17 ksi. The stress intensities occur directly under the point of load application.

4.2.3 The existing Pl value in the shell per the original CE Report (Paragraph 2.2.2.c) page 6 is 17.4 ksi which is also the existing (Pl + Pb) stress intensity.

4.2.4 The new value of Pm can be conservatively calculated as 17.4 + 0.09 = 17.49 ksi. The new value of Pl + Pb can be conservatively calculated as 17.57 ksi.

4.2.5 The allowable value of primary membrane is Sm, which equals 20 ksi and the allowable values of primary local (Pl) and primary local plus primary bending (Pl + Pb)are 1.5 Sm, which equals 30 ksi.

4.3 The force F2 is applied to the reactor pressure vessel (RPV) shell at 329.25 inches above the RPV 00 elevation with values same as F1 = 21.63 kips.

4.3.1 The same FE model as for F1 was used for the analysis.

4.3.2 From the FE model, Pl = 0.09 ksi & Pl + Pb = 0.17 ksi. These stress intensities occur directly under the point of load application. These stresses are localized and qualify as primary local stress Pl.

4.3.3 The existing Pl intensity due to this load per the original CE report (paragraph 2.2.2.c) page 6 is 17.4 ksi which is also the existing Pl + Pb stress intensity.

4.3.4 The new value of Pl can be conservatively calculated as 17.4 + 0.09 = 17.49 ksi. The new value of Pl + Pb is 17.57 ksi.

4.3.5 The allowable value of Pl is 1.5 Sm, which equals 30 ksi and the allowable value of primary local plus primary bending stress intensity is 1.5 Sm, which equals 30.0 ksi.

4.4 The force F3 = 63.8 kips is applied to the RPV shell at 176.25 inches above the RPV 00 elevation.

4.4.1 The FE model and results are shown in Figures 5, 6 & 7.

4.4.2 From the FE model, Pl = 0.3 ksi & Pl + Pb = 0.5 psi. These stress intensities occur directly under the point of load application. These stresses are localized and qualify as primary local stress Pl.

4.4.3 The existing Pl intensity due to this load per the original CE Report (paragraph 2.2.2.c) page 6 is 17.4 ksi which is also the existing Pl + Pb stress intensity for three lower springs which contact the clear shell.

4.4.3.1 The new value of Pl can be conservatively calculated as 17.4 + 0.3 = 17.7 ksi. The new value of Pl + Pb is 17.9 ksi.

4.4.3.2 The allowable value of Pl is 1.5 Sm which equals 30 ksi & the allowable value of Pl + Pb is also 1.5 Sm which equals 30 ksi.

4.4.4 The existing Pl intensity due to this load per the original CE Report (paragraph 2.2.2.c) page C-338 is 23.73 ksi (For operating pressure of 1000 psi),which is also the existing Pl + Pb stress intensity for the lower spring with contact bearing against the flare of the 270° recirculation outlet nozzle.

4.4.4.1 The new value of Pl can be conservatively calculated as 23.73 + 0.3 = 24.03 ksi. The new value of Pl + Pb is 23.73 + 0.5 = 24.23 ksi.

4.4.4.2 The allowable value of Pl is 1.5 Sm which equals 30 ksi & the allowable value of Pl + Pb is also 1.5 Sm which equals 30 ksi.

4.5 The stresses at the junction of the cone and the RPV due to loads F4 & F5 are evaluated using an ANSYS FE model and are found to be acceptable. These results are documented in 2.2.2.d.

4.6 All of the stress intensities due to the new design mechanical loads F1, F2, F3, F4 & F5 satisfy the allowable stress intensities of the original code of construction.

TABLE 1. ADDITIONAL DESIGN MECHANICAL LOADS

	SEISMIC + STEAM LINE LOCA	SEISMIC + LOCA RECIRCULATION LINE
F1+ F2	21.63 kips	21.63 kips
F_3	63.8 kips	63.8 kips
F4	Note 2	Note 2
F5	Note 2	Note 2

Notes: (1) F_1, F_2, and F_3 are discrete loads applied over a small area. At any one point in time, 1 F1, 1 F2 and 1 F3 are applied to one location. At any one point in time, F_4 is applied to 4 locations 90° apart for the installation of four shroud stabilizer assemblies. At any one point in time, F5 is applied to 6 locations 60" apart for the installation of six H8 weld brackets

(2) Numerical values and evaluation of stresses due to F4, F5 are given in 2.2.2.d.

(3) F1 + F2 total load is conservatively applied at both locations i:e. F1 = F2 = 21.63 kips for analysis purpose only.

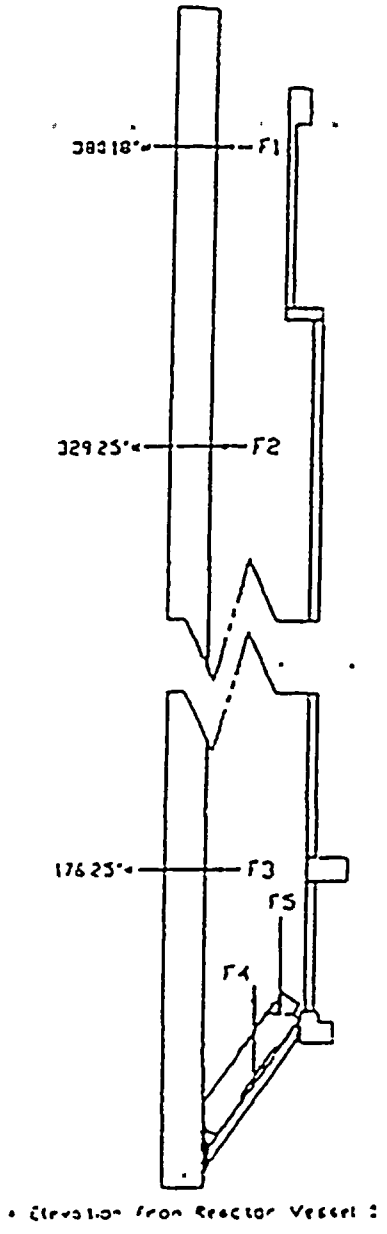

FIGURE 1. LOCATION OF DESIGN MECHANICAL LOADS

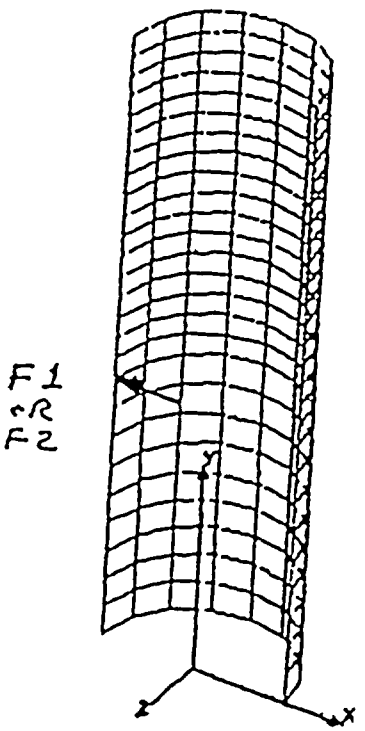

FIGURE 2. FEM FOR F1 or F2

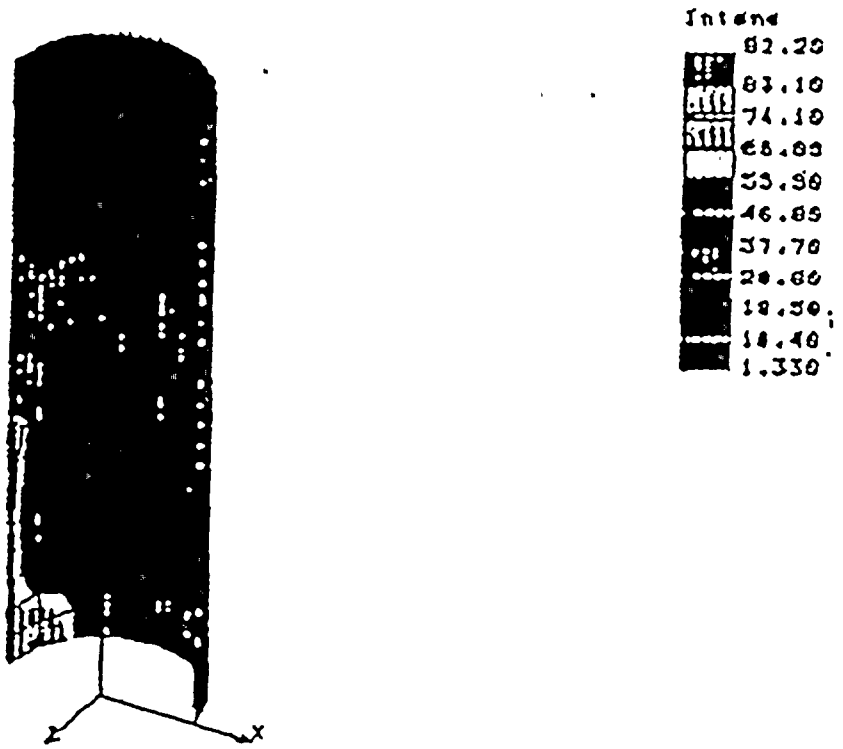

FIGURE 3. PI FOR F1 or F2

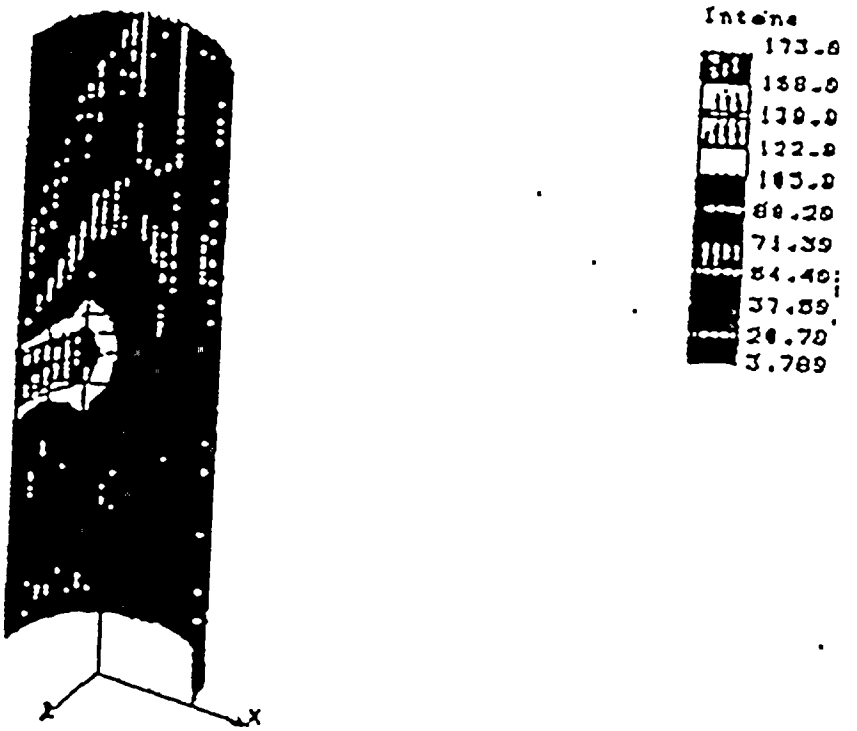

FIGURE 4. Pl ÷ Pb FOR F1 or F2

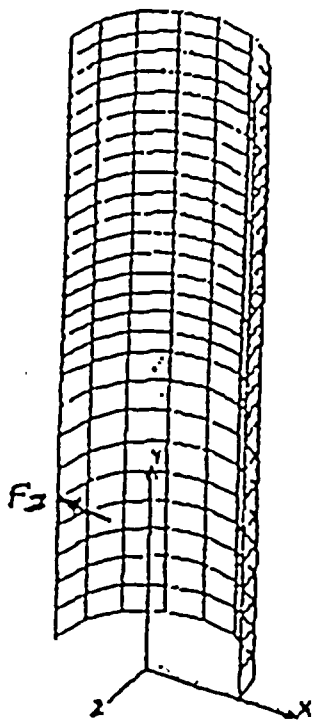

FIGURE 5. FEM FOR F3

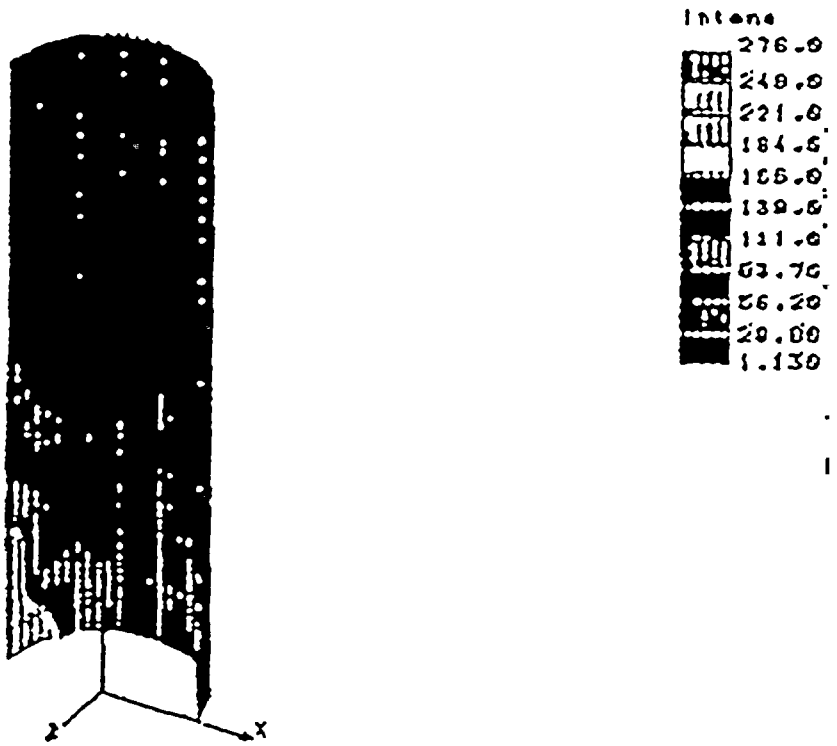

FIGURE 6. PI FOR F3

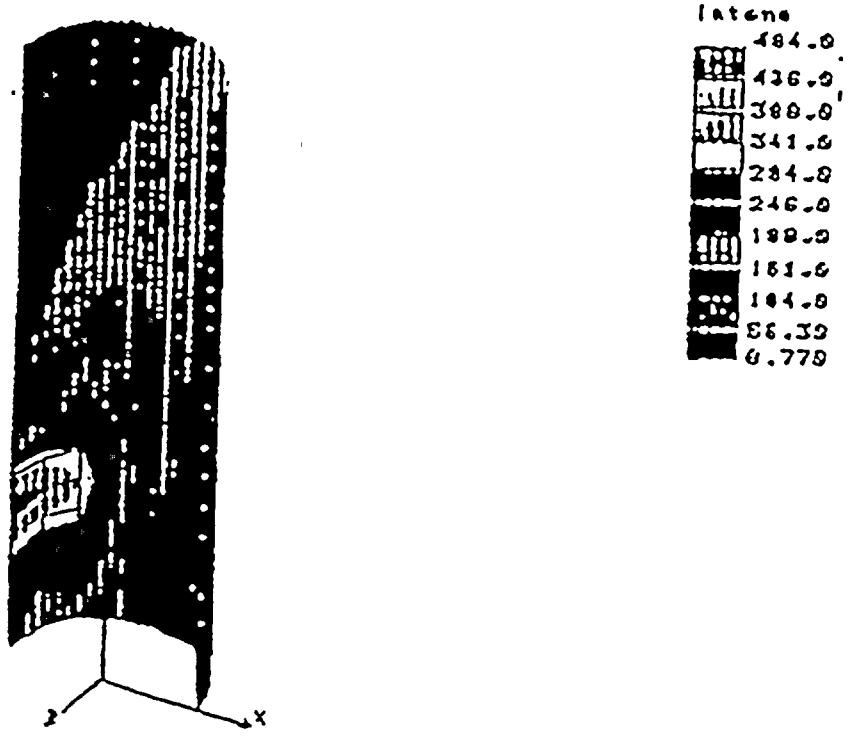

FIGURE 7. P1 ÷ Pb FOR F3

ATTACHMENT TO SPECIFICATION 24A6426
VESSEL BEARING STRESS EVALUATION

Introduction

This Attachment addresses the bearing stress which results from the modified placement of the spring against the vessel wall. With the modified placement, the area over which the reaction load is applied is reduced to approximately 1 square inch. The calculated bearing stresses are evaluated against the bearing stress requirements of the ASME Code Section III, NB-3227.1. The original vessel design basis documents do not include bearing stress acceptance criteria.

Description of Analysis

In this Attachment, an analysis is described which was performed to determine the bearing stress in the reactor pressure vessel material. In this analysis, the presence of the stainless steel vessel cladding was considered by applying the bearing load to this material, then determining how this load is transferred through the cladding and finally into the low alloy material.

A finite element analysis was performed to determine the dissipation of the stress through the cladding. The analysis was performed using the ANSYS finite element program. The model was axisymmetric about the applied loading area. The load was applied to a one square inch area. The vessel was modeled as a sphere. Figure III-1 shows the finite element model used in this analysis. A stainless steel clad of 0.219 inch was included in the model. Properties at operating temperatures were used in the analysis. The load was applied as a static load

Results

The results of the elastic analysis are shown in Figures III-2 and III-3. Figure III-2 shows the radial stress in the modeled portion of the vessel. Figure III-3 shows a close-up view of the model. As seen in Figure III-3, the applied stress in the direction of the loading distributes with depth into the cladding. The load carrying area at the vessel/clad interface has increased significantly compared to the clad surface contact area.

To determine the effect of the cladding on the average bearing stress, the average of the stress at the surface can be compared against that for the vessel/clad interface (with same area as surface contact area). In addition, a more realistic approach is to take the average stress over the area which is now subjected to stress at the vessel/clad interface. As shown in Figure III-3, there is a larger effective cross-sectional area which is now supporting the applied bearing load at the vessel/clad interface.

The average bearing stress at the surface is equal to 63 ksi. The average stress at the vessel\clad interface using the same cross-sectional-area is 55.9 ksi. However, when the area is modified to better represent the area withstanding the bearing load at the vessel\clad surface, the average stress is approximately 47.5 ksi. This demonstrates a 25% drop in the bearing stress.

Allowable Bearing Stresses

The ASME Code Section III, NB-3227.1, states that the bearing stress at temperature can be up to $1.5S_y$ (S_y=yield strength). Using a yield strength at temperature of 44.15 ksi, this gives an allowable stress of 66.22 ksi. As shown in the previous section, the bearing stress in the vessel material ranges from 55.9 ksi to 47.5 ksi depending on the load bearing cross-section assumption. Thus, the resulting bearing stress is below the maximum allowable stress.

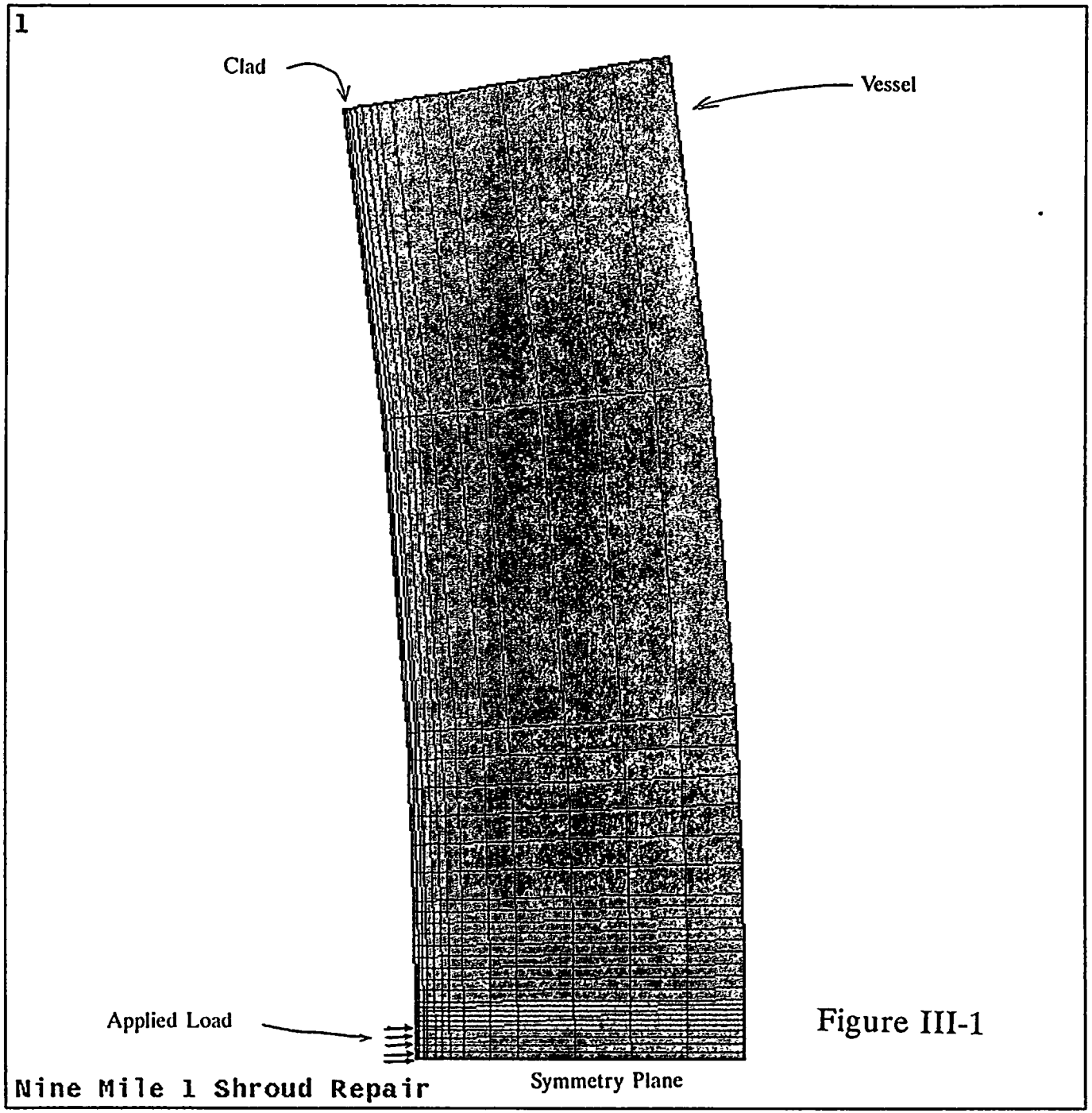
1
Clad
Vessel
Applied Load
Symmetry Plane
Nine Mile 1 Shroud Repair
ANSYS 4.4A1
APR 25 1996
8:16:02
POST1 ELEMENTS
MAT NUM
ZV =1
DIST=9.813
XF =108.826
YF =8.921

Figure III-1

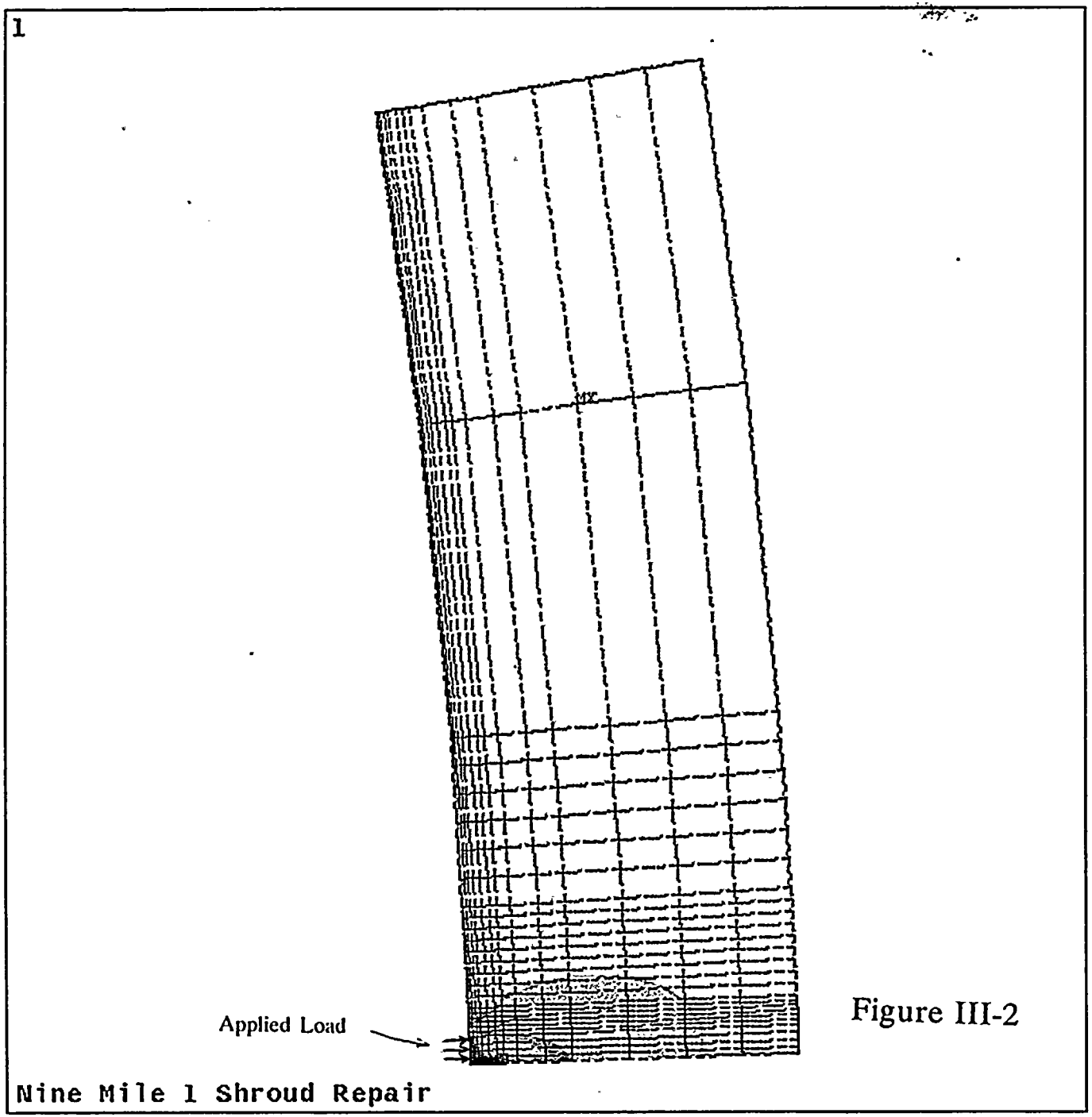
1
ANSYS 4.4A1
APR 23 1996
12:36:42
POST1 STRESS
STEP=1
ITER=1
SX (AVG)
S GLOBAL
DMX =0.204629
SMN =-69341
SMNB=-75108
SMX =2113
SMXB=13308
ZV =1
DIST=9.813
XF =108.826
YF =8.921
-69341
-61402
-53463
-45523
-37584
-29645
-21705
-13766
-5826
2113
Applied Load
Nine Mile 1 Shroud Repair

Figure III-2

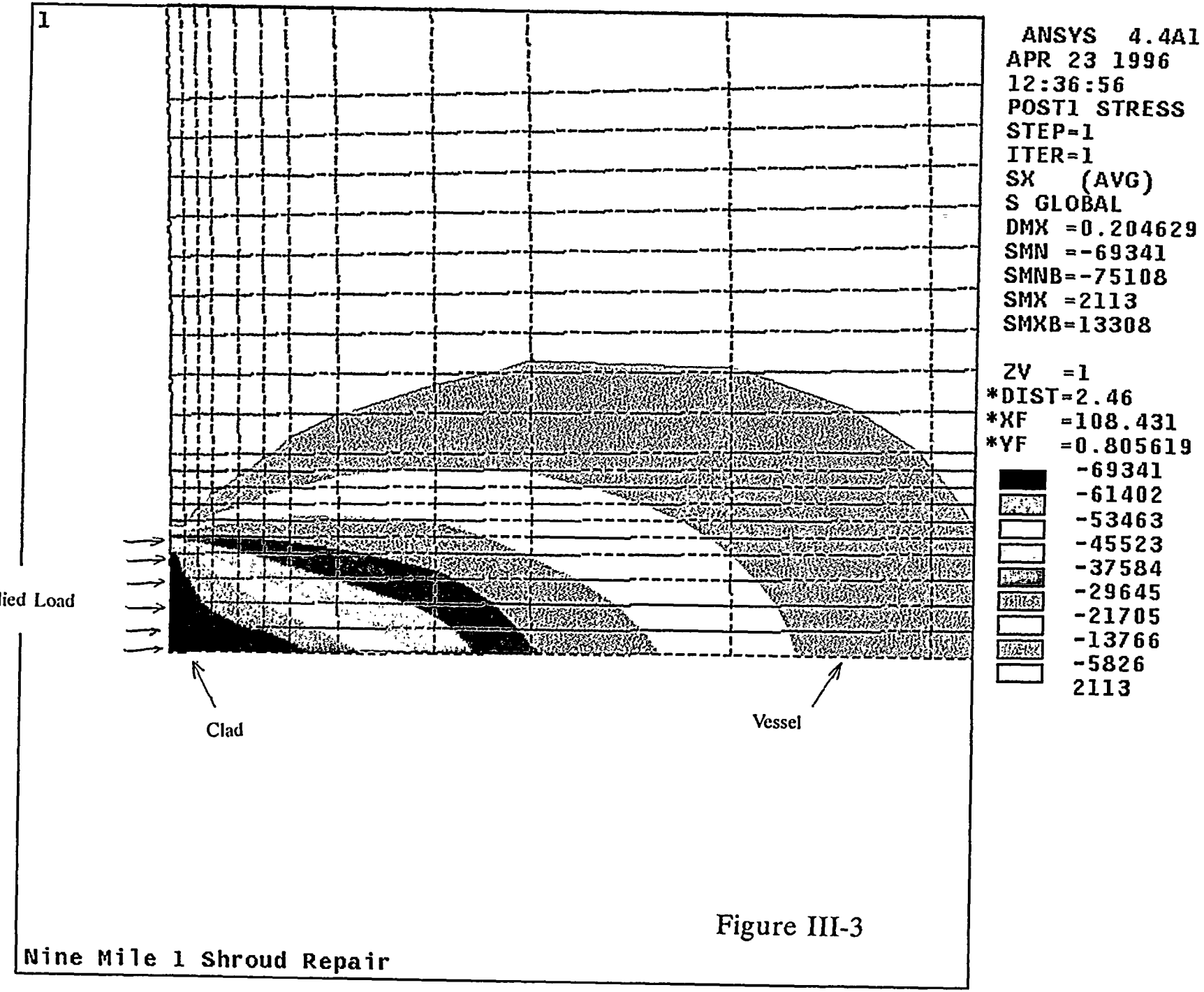
1
ANSYS 4.4A1
APR 23 1996
12:36:56
POST1 STRESS
STEP=1
ITER=1
SX (AVG)
S GLOBAL
DMX =0.204629
SMN =-69341
SMNB=-75108
SMX =2113
SMXB=13308
ZV =1
*DIST=2.46
*XF =108.431
*YF =0.805619
-69341
-61402
-53463
-45523
-37584
-29645
-21705
-13766
-5826
2113
Applied Load
Clad
Vessel
Nine Mile 1 Shroud Repair

Figure III-3

APPENDIX III

Description of the Improved Seismic Model

APPENDIX IV

Friction Factor Documentation

G160

GENERAL ENGINEERING LABORATORY

INVESTIGATION OF THE SLIDING BEHAVIOR OF A NUMBER OF ALLOYS UNDER DRY AND WATER LUBRICATED CONDITIONS

by

R. E. LEE, JR.

REPORT NO. 60GL20

JANUARY 22, 1960

GENERAL ELECTRIC

General Engineering Laboratory

INVESTIGATION OF THE SLIDING BEHAVIOR OF A NUMBER OF ALLOYS UNDER DRY AND WATER LUBRICATED CONDITIONS

by

R. E. Lee, Jr.

Report No. 60GL20 January 22, 1960

Knolls Atomic Power Laboratory, Operated
by General Electric Company for
the United States Atomic Energy Commission
Contract No. W-31-109 Eng-52

GENERAL ELECTRIC

SCHENECTADY, NEW YORK

INTRODUCTION

The object of this investigation was to study the sliding behavior of materials that are presently under consideration for use as components in a pressurized reactor. These materials, in addition to having to meet the physical and mechanical property requirements dictated by design considerations, must also adhere to friction and wear limitations, i.e., characteristics important to the insurance of satisfactory sliding performance under service conditions. In these areas where relative motion between mating surfaces occur, high friction, wear and surface damage in such forms as galling and scoring, can have a pronounced effect on the overall performance of the components during operation.

The results of these tests will provide information typical of two conditions under which relative motion will occur, namely, assembly (dry), and start up (200 F).

The first part of the program was devoted to studying the sliding behavior of typical structural materials in their conventional or uncoated state. The second part was carried out to determine what types of coatings would have sufficient protective properties to prevent galling and excessive wear between sliding members, when at least one of the members were coated.

CONCLUSIONS

Under the conditions tested:

1. The wear and surface damage of Inconel sliding against itself was considerably more severe than the austenitic AISI 304 stainless steel in combination with itself.

2. Replacing one of the Inconel-Inconel sliding members with Zircaloy 2, significantly reduced the wear and surface damage.

3. The application of protective coatings resulted in considerable improvement over that of the conventional (uncoated) material combinations. The coatings that proved effective in reducing the wear and surface damage of Inconel were:

   (a) Stellite 6 (overlay)

   (b) Colmonoy 6 (overlay)

   (c) Hard Chromium Plate (approx. 0.004 in. minimum)

TABLE OF CONTENTS

SUMMARY OF RESULTS

Conventional Materials

1. The 304 stainless steel in combination with itself performed with considerable less wear and at a lower coefficient of friction than the Inconel in combination with itself. At the light loads, the mode of surface damage (dry and lubricated) was essentially the same for both material combinations, differing only in magnitude from each other. At 1500 psi, the 304 stainless steel underwent moderate galling and some spalling, while the Inconel suffered heavy plastic deformation and galling. Figures 1 and 2 clearly indicate the significant difference in sliding behavior between the two combinations under identical test conditions. The damage incurred on each corresponding flat surface was similar in nature and magnitude to that of the damage observed on the slider surfaces.

2. In comparing Zircaloy 2 in combination with Inconel and 304 stainless steel, it was noted at the lower loads the performance of both combinations were quite comparable. At the 1500 psi load, in deoxygenated water, the Inconel-Zircaloy 2 combination performed quite well and with less wear resulting than with the 304 stainless steel-Zircaloy 2 combination under the same conditions. Figures 3 and 4 each show the wear track of a Zircaloy 2 flat, generated by an Inconel, and 304 stainless steel slider respectively, in 200 F deoxygenated water at a load of 1500 psi.

3. At the light loads, i.e. 100 psi, the performance of 304 stainless steel in combination with Inconel fell approximately half way between the performance of the Inconel vs. Inconel and 304 stainless steel vs. 304 stainless steel combinations under identical test conditions.

4. Table 1 summarizes the significant results of the uncoated structural materials, and Table 3 gives a detailed description of these tests.

Coated Materials

5. A (puddled) Stellite 6 coating, approximately .030 inches thick applied on Inconel in combination with Inconel, proved to be one of the outstanding performers in deoxygenated water at 200 F. At the light load only faint traces of a wear track could be observed on the Stellite 6 surface. At the higher load, i.e. 1500 psi, polishing was observed and wear was very low. Figure 5 shows the wear track made by an Inconel slider on a Stellite 6 coating. Slider wear was low.

6. Inconel in combination with Colmonoy 6 plated Inconel performed satisfactory in 200 F deoxygenated water, at the low load, i.e. 100 psi, but at the higher load the Inconel slider surface commenced to become galled and deeply grooved. The Colmonoy surface on the other hand was only lightly galled and wear was practically nil.

7. Inconel, sliding on chromium plated Inconel, and 304 stainless steel sliding on chromium plated stainless steel, indicated good sliding characteristics under dry and water lubricated conditions at both low and high loads. These combinations were quite comparable to one another in performance. The improvement was considerable over that of sliding on themselves in the uncoated conditions, especially in the case of the Inconel-Inconel combination. Figure 6 shows the wear track on a chromium plated Inconel flat, made by an Inconel slider. Figure 7 shows the wear track on a chromium plated 304 stainless steel flat made by a 304 stainless steel slider. The friction incurred at each load level for both combinations, was fairly comparable as was the dry and water lubricated friction results. See Table 2. It was interesting to note, however, that for both chromium plated combinations, their general performance was slightly better in deoxygenated water than under dry sliding conditions. The chromium wear tracks were highly polished from the water tests while in dry sliding (in air), they had a dark gray to black, rough surface appearance. A plausible explanation for this behavior is that oxidation was taking place rapidly in air and, therefore, part of the oxidized wear product from the chromium, and Inconel or 304 stainless steel, was transferred to the sliding surfaces. This then gave the appearance of a dark to black rough surface. The water tests, on the other hand, were conducted in deoxygenated water and were relatively free from oxygen, thus preventing any significant oxidation from taking place.

8. The Electrolized plating on Inconel, in combination with Inconel, gave a fairly good performance at the light load under the conditions tested, but the plating was quickly removed at the higher load. Figure 8 shows the magnitude of damage observed at the 1500 psi load level.

9. The Electroless, and Electrolytic nickel coatings on Inconel proved to have undesirable sliding characteristics under the conditions tested. Wear was comparable to the uncoated Inconel-Inconel combination at the low loads, and there was considerable evidence of metal pickup and welding.

10. Table 2 summarizes the significant results of the coated material sliding tests and Table 4 gives a detailed description of these tests.

Table 1

SIGNIFICANT RESULTS

Conventional Materials

Specimens		Coefficient of Friction (Avg.) (μ)				Overall Wear (mils)			
		Dry Lub		Deoxygenated Water		Dry Lub		Deoxygenated Water	
Slider	Flat	100 psi	1500 psi	100 psi	1500 psi	100 psi	1500 psi	100 psi	1500 psi
Zircaloy 2	Inconel	0.49		0.37	0.42	+0.6		-0.2	-0.6
Zircaloy 2	304 Stainless Steel	0.40		0.59	0.44	-0.5		+0.4	-4.3
304 Stainless Steel	304 Stainless Steel	0.40	0.44	0.59	0.48	-0.7	-2.5	-0.2	+0.7
Inconel	Inconel	0.80	0.74	0.58	0.70	-4.2	-50.0[1]	-4.9	-55.0

[1]Suspended test at 1400 cycles - excessive wear

Table 2

SIGNIFICANT RESULTS

Coated Materials

Specimens		Coefficient of Friction (Avg.)				Overall Wear			
		Dry Lub (μ)		Deoxygenated Water (μ)		Dry Lub (mils)		Deoxygenated Water (mils)	
Slider	Flat	100 psi	1500 psi	100 psi	1500 psi	100 psi	1500 psi	100 psi	1500 psi
Inconel	Stellite 6 on Inconel			0.63	0.49			-0.4	-0.3
304 Stainless Steel	Chromium Plate on 304 Stainless Steel	0.62	0.50	0.66	0.53	+0.1	-1.4	-0.1	-0.1
Inconel	Chromium Plate on Inconel	0.62	0.44	0.58	0.42	-0.1	+0.5	+0.2	+0.1
Inconel	Colmonoy on Inconel			0.65	0.49			-0.1	+0.1

TABLE 3

SLIDING TESTS

TEST NO	SLIDER	FLAT	FINISH SLIDER	FINISH FLAT	LOAD	TOTAL CYCLES	TEMP °F	DATE RUN	FRICTION COEFFICIENT start	FRICTION COEFFICIENT last	FRICTION COEFFICIENT min	FRICTION COEFFICIENT max	FRICTION COEFFICIENT ave.	Wear Overall mils	Wear Slider mils	Travel in.	Lab.	DAMAGE SLIDER	DAMAGE FLAT
1	INCONEL	INCONEL	8-10	3-5	100 psi	2000	74	5/21/59	.83	.83	.83	.74	.85	.80	-1.2	-1.7	2000	DAY	HEAVY GALLING, METAL PICKUP - PLOUGHING	HEAVY GALLING - METAL PICKUP - WELL DEFINED WEAR AREA
2	INCONEL	INCONEL	8-10	3-5	100 psi	2000	200	5/4/59	.28	.28	.26	.28	.26	.58	-4.9	-2.0	2000	DANIELSON WATER	HEAVY GALLING - SOME METAL PICKUP	HEAVY GALLING - METAL PICKUP - PLOUGHING - WELL DEFINED WEAR AREA
3	ZIRCALOY 2	INCONEL	16-21	3-5	100 psi	2000	74	5/22/59	.55	.38	.46	.46	.52	.49	+0.6	+0.8	2000	DAY	HEAVY GALLING AND METAL PICKUP - CONSIDERABLE PLOUGHING	HEAVY GALLING AND METAL PICKUP - PLOUGHING
4	ZIRCALOY 2	INCONEL	16-21	3-5	100 psi	2000	200	5/15/59	.28	.28	.44	.38	.44	.37	-0.2	10.2	2000	DANIELSON WATER	MODERATE SCORING	WEAR NIL - POLISHED SURFACE SEVERAL LIGHT SCRATCHES
6	430 STAINLESS STEEL	INCONEL	18-22	3-5	100 psi	2000	74	5/22/59	.18	.18	.32	.18	.33	.50	-3.3	-1.8	2000	DAY	MODERATE TO HEAVY GALLING	MODERATE TO HEAVY GALLING - METAL PICKUP - SOME PLOUGHING
8	304 STAINLESS STEEL	INCONEL	12-19	3-5	100 psi	2000	74	5/25/59	.60	.60	.66	.66	.90	.25	-1.2	+0.2	2000	DAY	LIGHT TO MODERATE GALLING	MODERATE TO HEAVY GALLING - CONSIDERABLE METAL PICKUP
21	304 STAINLESS STEEL	304 STAINLESS STEEL	12-19	6-13	100 psi	2000	74	5/27/59	.26	1.26	.25	.26	.27	.20	-0.7	+0.1	2000	DAY	MODERATE GALLING - LIGHT PICKUP - LOW WEAR	LIGHT TO MODERATE GALLING - LIGHT PICKUP - LOW WEAR
22	304 STAINLESS STEEL	304 STAINLESS STEEL	12-19	6-13	100 psi	2000	200	5/28/59	.59	.53	.66	.55	.76	.59	-0.2	0	2000	DANIELSON WATER	MODERATE SCORING - NO MEASURABLE WEAR	LIGHT GALLING - LOW WEAR
25	ZIRCALOY 2	304 STAINLESS STEEL	16-21	6-13	100 psi	2000	74	6/4/59	.21	.21	.51	.21	.51	.10	-0.5	+0.2	2000	DAY	MODERATE GALLING - LOW WEAR	LIGHT GALLING - MODERATE SCORING - LOW WEAR
26	ZIRCALOY 2	304 STAINLESS STEEL	16-21	6-13	100 psi	2000	200	5/18/59	.52	.52	.76	.50	.87	.59	+0.4	+0.3	2000	DANIELSON WATER	MODERATE SCORING AND GALLING - LOW WEAR	LIGHT TO MODERATE GALLING - WEAR NIL
30	INCONEL X	INCONEL	7-10	3-5	100 psi	2000	200	5/20/59	.85	.83	.83	.83	.87	.84	-3.2	-0.8	2000	DANIELSON WATER	MODERATE GALLING - CONSIDERABLE PICKUP	LIGHT TO MODERATE GALLING
31	INCONEL X	INCONEL	7-10	3-5	100 psi	2000	74	5/20/59	.76	.76	.74	.74	.77	.76	-2.7	-1.1	2000	DAY	MODERATE PICKUP AND GALLING	MODERATE TO HEAVY GALLING CONSIDERABLE PICKUP
5	304 STAINLESS STEEL	304 STAINLESS STEEL	12-19	6-13	1500 psi	2000	74	6/4/59	.35	.39	.48	.39	.53	.44	-2.5	-1.6	2000	DAY	LIGHT GALLING AND PICKUP - GROOVED AREAS	MODERATE GALLING AND PICKUP - GROOVED AREAS
7	304 STAINLESS STEEL	304 STAINLESS STEEL	12-19	6-13	1500 psi	2000	200	6/5/59	.50	.50	.46	.45	.51	.48	10.7	+0.1	2000	NORTON WATER	SPALLED AND GROOVED AREAS - SOME MATERIAL EMBED ON SURFACE	SPALLED AND GROOVED AREAS - LIGHT SCORING DISCOLORATION ON TRACK
10	INCONEL	INCONEL	8-10	3-5	1500 psi	[illegible] WEAR	74	6/5/59	.78	.78	.81	.69	.81	.24	-50.0	-31.5	1400	DAY	EXTREMELY HEAVY PLASTIC DEFORMATION AND GALLING EXCESSIVE WEAR	EXTREMELY HEAVY PLASTIC DEFORMATION AND GALLING EXCESSIVE WEAR
27	INCONEL	INCONEL	8-10	3-5	1500 psi	2000	200	6/8/59	.81	.81	.63	.61	.81	.70	-55.0	-48.0	2000	DANIELSON WATER	EXTREMELY HEAVY GALLING EXCESSIVE WEAR	EXTREMELY HEAVY GALLING EXCESSIVE WEAR
9	304 STAINLESS STEEL	INCONEL	12-19	3-5	100 psi	2000	200	5/15/59	.35	.28	.42	.28	.63	.56	+0.6	+0.1	2000	DANIELSON WATER	CONSIDERABLE PICKUP AND GALLING	CONSIDERABLE PICKUP AND GALLING
28	ZIRCALOY 2	304 STAINLESS STEEL	16-21	6-13	1500 psi	2000	200	6/19/59	.40	.31	.41	.31	.49	.44	-4.3	-2.7	2000	NORTON WATER	MODERATE GALLING	UNIFORM WEAR
35	ZIRCALOY 2	INCONEL	16-21	3-5	1500 psi	2000	200	6/18/59	.42	.38	.45	.38	.45	.42	-0.6	-0.1	2000	DANIELSON WATER	MODERATE GALLING - SOME GROOVING AND PICKUP - LOW WEAR	LOW WEAR - LIGHT SCALE OF MODERATE SCORING POLISHED SCRATCHES

TABLE I

ALLOWED TESTS

TEST NO	SLIDER	FLAT	FINISH SLIDER	FINISH FLAT	LOAD PSI	TOTAL CYCLES	TEMP °F	DATE RUN	FRICTION COEFFICIENT f start	f init	f fin	f min	f max	f ave	WEAR OVERALL mils	SLIDER WEAR mils	TRAVEL in.	LUB:	DAMAGE SLIDER	DAMAGE FLAT
11	INCONEL	CHROMIUM PLATE ON INCONEL	8-10	.1-1.2	100	2000	74	6/11/59	.51	.57	.73	.55	.73	.62	-.1	NOT MEASURABLE	2000	DRY	SOME PICKUP OF CHROMIUM. WEAR NIL	SMOOTH SURFACE-WEAR NIL PLATING INTACT - INITIAL PLATING .001"
12	INCONEL	CHROMIUM PLATE ON INCONEL	8-10	.1-1.2	100	2000	200	6/13/59	.61	.55	.62	.55	.62	.58	+.2	-.1	2000	DEMIN. WATER	SMOOTH SURFACE WEAR LOW	POLISHED - WEAR NIL INITIAL PLATING .0038"
13	INCONEL	ELECTROPLATED INCONEL	8-10	5-15	100	2000	74	6/11/59	.52	.52	.55	.51	.59	.56	-.1	NOT MEASURABLE	2000	DRY	MINIMUM PICKUP AND GALLING	LIGHT SCORING - WEAR LOW INITIAL PLATING .0001"
14	INCONEL	ELECTROPLATED INCONEL	8-10	5-15	100	2000	200	6/13/59	.58	.58	.61	.58	.65	.61	-.1	NOT MEASURABLE	2000	DEMIN. WATER	WEAR NIL	POLISHED - WEAR NIL INITIAL PLATING .0301"
15	INCONEL	ELECTROLESS NICKEL PLATE ON INCONEL	8-10	13-27	100	2000	74	6/12/59	.84	.84	.53	.42	.84	.64	-.3	+.2	2000	DRY	METAL PICKUP WELDED ISLANDS	PLATING INTACT - WELDED ISLANDS FROM PICKUP INITIAL PLATING .0038"
16	INCONEL	ELECTROLESS NICKEL PLATE ON INCONEL	8-10	13-27	100	2000	200	6/16/59	.64	.64	.55	.46	.64	.56	-1.0	+.2	2000	DEMIN WATER	GROOVED CONSIDERABLE	METAL PICKUP - LARGE ISLANDS OF WELD METAL INITIAL PLATING .0138"
17	INCONEL	ELECTROLYTIC NICKEL PLATE ON INCONEL	8-10	2-11	100	2000	74	6/11/59	.75	.75	.72	.63	.75	.73	+.1	+.2	2000	DRY	METAL PICKUP SOME SCORING	LOW WEAR - PLATING INTACT INITIAL PLATING .0037
18	INCONEL	ELECTROLYTIC NICKEL PLATE ON INCONEL	8-10	.2-11	100	2000	200	6/14/59	.66	.53	.78	.53	.78	.70	-.7	+.3	2000	DEMIN. WATER	PICKUP AND GALLING	METAL PICKUP - ISLANDS OF WELD INITIAL PLATING .004"
19	INCONEL	STELLITE 6 ON INCONEL	8-10	3-8	100	2000	200	6/3/59	.54	.54	.61	.54	.73	.63	-.4	NOT MEASURABLE	2000	DEMIN WATER	SMOOTH-WEAR NIL	EXCELLENT - FAINT TRACE OF WEAR TRACK INITIAL PLATING .030"
20	INCONEL	COLMONOY ON INCONEL	8-10	2.5-35	100	2000	200	6/3/59	.54	.54	.69	.54	.69	.65	-.1	NOT MEASURABLE	2000	DEMIN. WATER	WEAR NIL	POLISHED - WEAR NIL INITIAL PLATING .110"
23	304 STAINLESS STEEL	CHROMIUM PLATE ON 304 STAINLESS STEEL	12-14	1.5-2.5	100	2000	74	6/10/59	.26	.26	.79	.26	.83	.62	+.1	-.1	2000	DRY	LIGHT SCORING SOME PICKUP	SOME POLISHING-WEAR NIL INITIAL PLATING .0037"
24	304 STAINLESS STEEL	CHROMIUM PLATE ON 304 STAINLESS STEEL	12-14	1.5-2.5	100	2000	200	6/11/59	.57	.57	.72	.57	.72	.66	-.1	NOT MEASURABLE	2000	DEMIN WATER	POLISHING-WEAR NIL	POLISHING-WEAR NIL INITIAL PLATING .0034"
25	INCONEL	STELLITE 6 ON INCONEL	8-10	.3-8	1500	2000	200	6/16/59	.39	.39	.55	.39	.55	.49	-.3	NOT MEASURABLE	2000	DEMIN WATER	SOME PICKUP	POLISHING - WEAR NIL INITIAL PLATING .030"
33	INCONEL	COLMONOY ON INCONEL	8-10	2.5-35	1500	2000	200	6/18/59	.43	.43	.52	.43	.52	.49	+.1	-.1	2000	DEMIN WATER	DEEP GROOVING, HEAVY GALLING AND PICKUP	LIGHT GALLING - LOW WEAR INITIAL PLATING .030"
34	INCONEL	ELECTROLESS NICKEL PLATE ON INCONEL	8-10	13-27	1500	1000	74	6/17/59	.61	.61	.58	.55	.61	.58	-8.9	-5.0	1000	DRY	SEVERE GALLING EXCESSIVE WEAR	SEVERE GALLING - EXCESSIVE WEAR INITIAL PLATING .0038"
36	INCONEL	ELECTROLYTED INCONEL	8-10	5-15	1500	500	74	6/17/59	.78	.78	.74	.74	.78	.76	-13.0	-7.1	500	DRY	SEVERE GALLING EXCESSIVE WEAR	SEVERE GALLING-EXCESSIVE WEAR INITIAL PLATING .0031"
37	INCONEL	CHROMIUM PLATE ON INCONEL	8-10	.2-12	1500	2000	74	6/15/59	.43	.43	.59	.39	.59	.47	+.5	-.3	2000	DRY	PICKUP OF CHROMIUM LIGHT GALLING	SMOOTH SURFACE-UNIFORM WEAR-TRACE OF CHROME INITIAL PLATING .004
38	INCONEL	CHROMIUM PLATE ON INCONEL	8-10	.2-12	1500	2000	200	6/17/59	.48	.48	.39	.39	.49	.42	+.1	0	2000	DEMIN-GEN. WATER	SOME GROOVING, LIGHT CHROMIUM PICKUP - POLISHING	POLISHING - LIGHT SCORING PLATING INTACT LOW WEAR INITIAL PLATING .0038"
39	304 STAINLESS STEEL	CHROMIUM PLATE ON 304 STAINLESS STEEL	12-14	1.5-2.5	1500	2000	74	6/16/59	.39	.39	.51	.39	.51	.50	-1.4	-1.6	2000	DRY	LIGHT SCORING AND PICKUP	GRAY BURNISHED SURFACE, LIGHT PICKUP, LOW WEAR PLATING INTACT - PLATING .0032"
40	304 STAINLESS STEEL	CHROMIUM PLATE ON 304 STAINLESS STEEL	12-14	1.5-2.5	1500	2000	200	6/15/59	.43	.43	.53	.43	.57	.53	-.1	0	2000	DEMIN-GEN HANA	SOME SCORING WEAR NIL	POLISHED - SEVERAL LIGHT SCORE MARKS, PLATING INTACT, INITIAL PLATING .0034"

APPARATUS AND PROCEDURE - DESCRIPTION

(Test Conditions - see pg. 12)

The tests were conducted on a wear test apparatus in which a 3/4 inch slider with a truncated end consisting of a 13/64 inch diameter surface, was mounted in a reciprocating arm, and moved relative to the surface of a stationary 2 inch long by 1/2 inch wide by 1/4 inch thick flat specimen, at a velocity of 1 1/2 ft/min. One end of the arm was so mounted that the free end was able to move in either a vertical or horizontal plane. See Figure 9 for a photograph of the apparatus.

Sliding was obtained by moving the arm back and forth by means of an air actuated piston. To measure static and kinetic friction, the piston was disconnected and the arm was moved manually. A rod located at the end of the arm was instrumented with strain gages so that the friction force could be continuously recorded when so desired.

Measurements, consisting of change in height of lever arm, and change in length of truncated slider, were made for each run. The change in height was reported as overall wear since it contained the combined wear of both slider and flat. The height of the arm above the base plate was measured at several fixed positions with a dial indicator which was rigidly fastened to the base plate. Heat was supplied by resistance heaters in contact with the bottom of the flat. The flat specimen which was held stationary on a supporting table, was housed within an enclosure which could hold a lubricant. The top half of the enclosure surrounded the slider specimen and was fastened to the moving arm. This allowed for better control of argon gas blanketing and heating. The temperature was measured by a thermocouple clamped in proximity to the surface of the flat. The sliding tests run in deoxygenated water at 200°F had argon gas introduced under positive pressure into the enclosed test area to prevent the influx of oxygen. Argon was bubbled into the water reservoir of the test enclosure and simultaneously brought in through another inlet to blanket the surface of the water. Gas was also bubbled into the water supply. A front view schematic diagram of this setup can be seen in Figure 10. Prior to testing, the specimens were washed with soap and water, and rinsed in alcohol to eliminate any oil or other types of contaminant films.

After cleaning, the specimens were mounted in the apparatus and brought to the desired operating temperature under load. The height of the arm above the base plate was measured. The arm was moved manually for the first few cycles while static and kinetic friction were continuously recorded. The air actuated cylinder was then engaged to move the arm. A counter connected to the air actuated piston arm recorded the number of cycles. The slider moved 18 cycles/min for a total displacement of 18 inches or 1 1/2 ft/min. At the conclusion of 2000 cycles, the height of the arm was again measured and the test concluded. Macroscopic, and microscopic examination (at 12X and 36X) were made of the specimens upon completion of each test. Photographs were taken at 10X magnification of several tested specimens whose resulting wear surfaces were considered to be of special interest.

DEFINITION OF TEST TERMS

Finish	Average surface roughness (microinches)
Load	Unit loading on a 13/64 inch diameter slider specimen surface
Cycles	Tests were conducted at 18 cycles/minute where each cycle consisted of a reciprocating movement of two 1/2" strokes making the total displacement 18 inches/minute. The test duration was for 2000 cycles except in the case of excessive wear or coating failure.
Temperature	Temperature at which tests were conducted were: 74°F - unlubricated 200°F - bulk water (deoxygenated) temperature argon gas was introduced under positive pressure into the water reservoir and inclosed test area to prevent influx of oxygen. LiOH was added to the water resulting in a pH of 9.5-10.5
Friction Coefficient	f_{static} - initial coefficient of static friction taken at start of test
	$f_{initial}$ - initial kinetic coefficient of friction taken at start of test
	f_{final} - final kinetic coefficient of friction taken at end of 2000 cycle run
	f_{min} - lowest kinetic coefficient of friction recorded throughout test
	f_{max} - highest kinetic coefficient of friction recorded throughout test
	f_{avg} - average kinetic coefficient of friction values measured throughout test

Friction readings were taken at the following intervals throughout the test:

Initial, 50, 500, 1000 and 2000 cycles

Wear

Overall wear was measured at the end of each test. The overall wear was measured by means of a dial indicator that read to within 0.0001 inches, and was taken with the test specimen surfaces in actual contact. Slider wear was determined by measuring the slider length before and after each test.

Plus (+) indicates material buildup on the surface due to deformation and/or material transfer.
Minus (-) indicates material loss from the surface or surfaces due to wear and/or surface damage.

LIST OF FIGURES

APPENDIX

Material	Nominal Composition %	Configuration	Hardness [1] KHN	Hardness Rockwell
Inconel	77.0 Ni, 15.0 Cr, 7.0 Fe, 0.25Cu, 0.25 Si 0.25 Mn, 0.06 C, 0.007 S	Slider Flat	294 229	28C 96B
AISI 304 Stainless Steel	19.0 Cr, 9.5 Ni, 2.0 Mn, 1.0 Si, 0.16 C	Slider Flat	274 226	24C 95B
Zircaloy 2	1.5 Sn, 0.1 Fe, 3.0 Ni, 0.1 Cr, Bal Zr	Slider	263	22C
Inconel X	73.0 Ni, 15.0 Cr, 7.0 Fe, 0.05 Cu, 0.40 Si, 0.75 Al, 0.50 Mn, 0.05 C, 0.007 S, 2.50 Ti, 0.90 Cb + Ta	Slider	439	43C
AISI 4340 Steel	0.40 C, 0.70 Mn, 0.28 Si, 1.80 Ni, 0.80 Cr, 0.25 Mo, 0.040 S, 0.040 P	Slider	343	34C
Chromium Plate		Chromium Plate on Inconel Flat	805	63C
Chromium Plate		Chromium Plate on AISI 304 SS Flat	835	65C
Stellite 6 Overlay	28.0 Cr, 4.0 W, 1.0 C, Bal Co	Stellite 6 Overlay on Inconel Flat	581	52C
Colmonoy 6 Overlay	13.0-20.0 Cr, 2.75-4.0 Cr, 65.0-75.0 Ni, 10.0 Mn_{max}, Fe, C	Colmonoy 6 Overlay on Inconel Flat	805	63C
Electrolize Coating	Chromium Alloy - Proprietary	Electrolize On Inconel Flat	477	46C
Electroless Nickel Plate (Kanigen)	90.0-92.0 Ni, 8.0-10.0 P, 0.040 C, 0.0023 O_2, 0.0047 N_2, 0.0016 H_2	Nickel Plate On Inconel Flat	563	51C
Electrolytic Nickel Plate		Nickel Plate On Inconel Flat	567	52C

[1] Knoop hardness measurements were made on a Tukon Hardness Tester using a 1 Kg load, and 20X objective. The only exception was the Electrolize coating whose hardness was measured at a 200 gm load. The Rockwell hardness values were obtained from conversion tables.

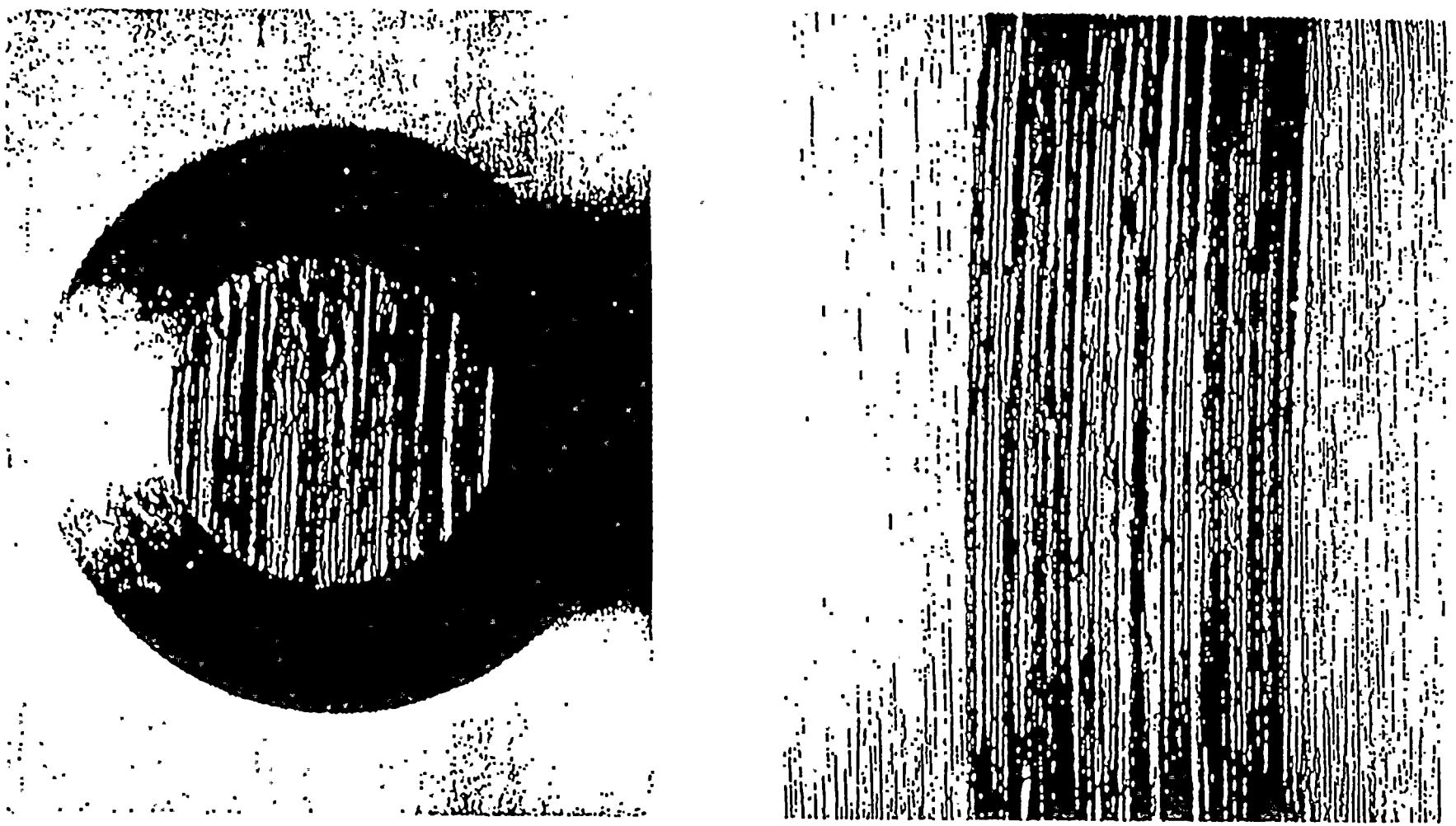

Slider

Flat

Fig. 1. AISI 304 Stainless Steel vs AISI 304 Stainless Steel - Test 7.

Load	-	1500 psi
Lubricant	-	Deoxygenated water
Temperature	-	200 F
Period	-	2000 cycles

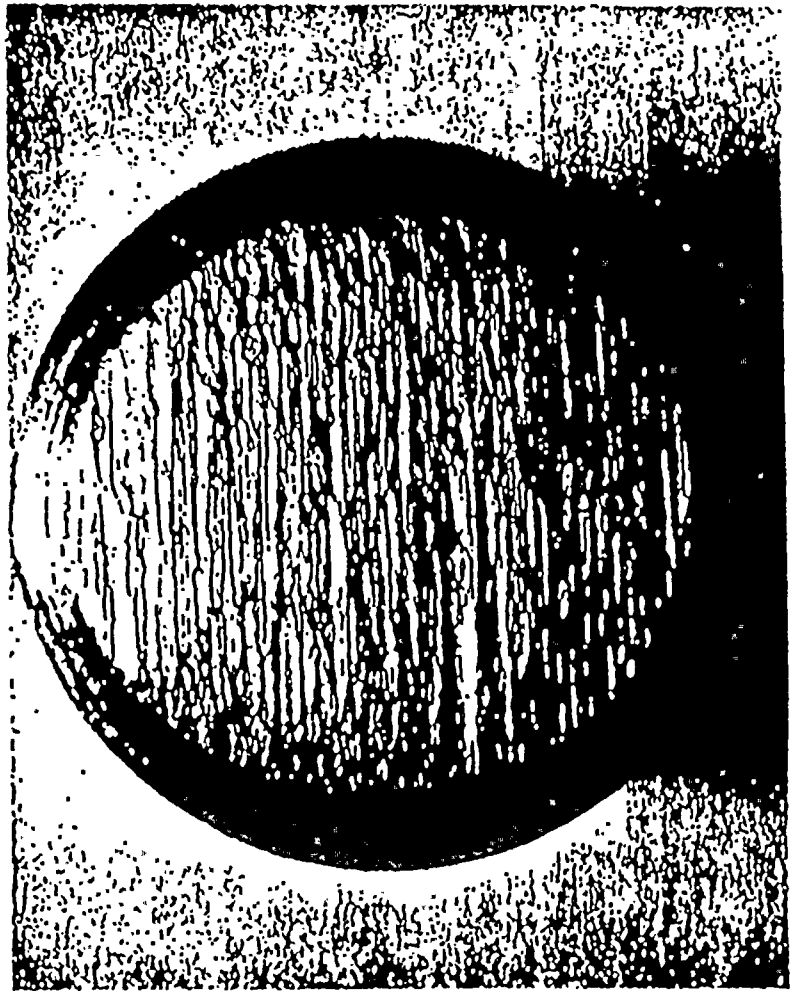

Slider

Flat

Fig. 2. Inconel vs. Inconel - Test 27.
Load - 1500 psi
Lubricant - Deoxygenated water
Temperature - 200 F
Period - 2000 cycles

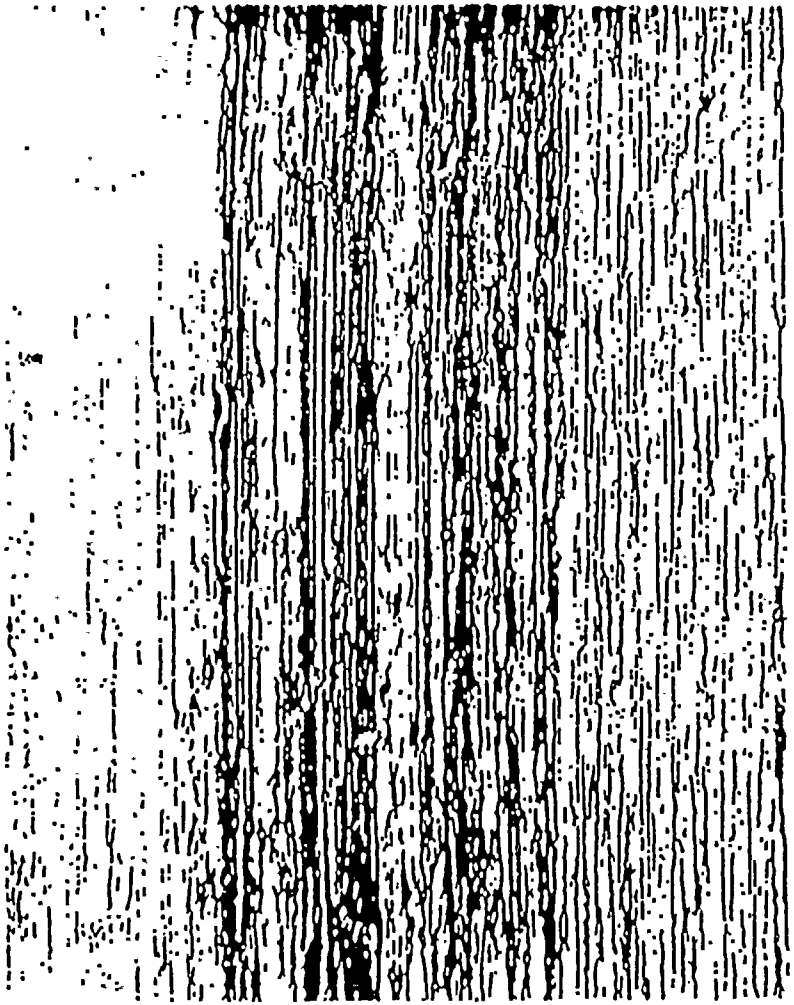

Fig. 3. Inconel flat wear track. Slider was Zircoloy 2 - Test 35.

Load	- 1500 psi
Lubricant	- Deoxygenated water
Temperature	- 200 F
Period	- 2000 cycles

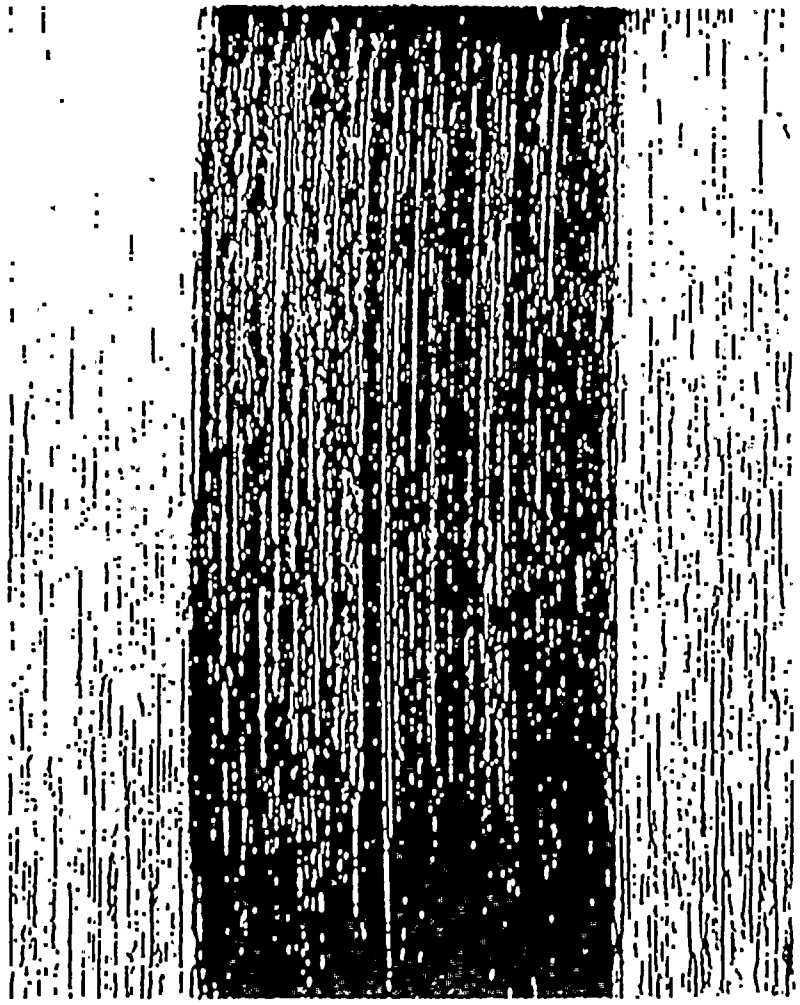

Fig. 4. AISI 304 Stainless Steel flat wear track. Slider was Zircoloy 2. Test 28.

Load	- 1500 psi
Lubricant	- Deoxygenated water
Temperature	- 200 F
Period	- 2000 cycles

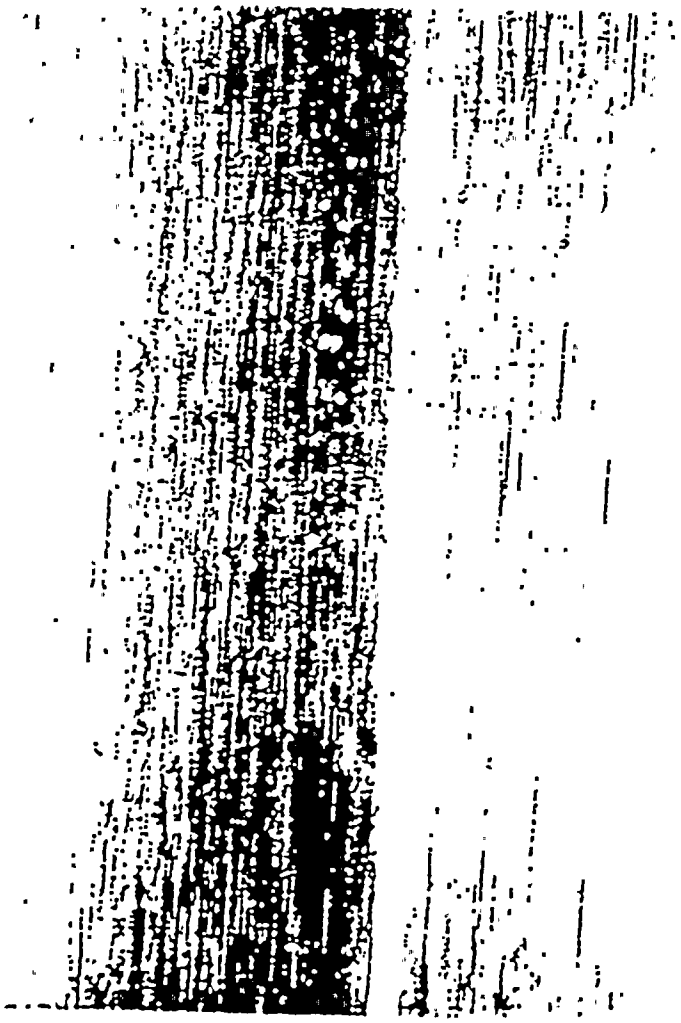

Fig. 5. Wear track of Stellite 6 coated Inconel. Slider material was Inconel - Test 29.

Load	- 1500 psi
Lubricant	- Deoxygenated water
Temperature	- 200 F
Period	- 2000 cycles

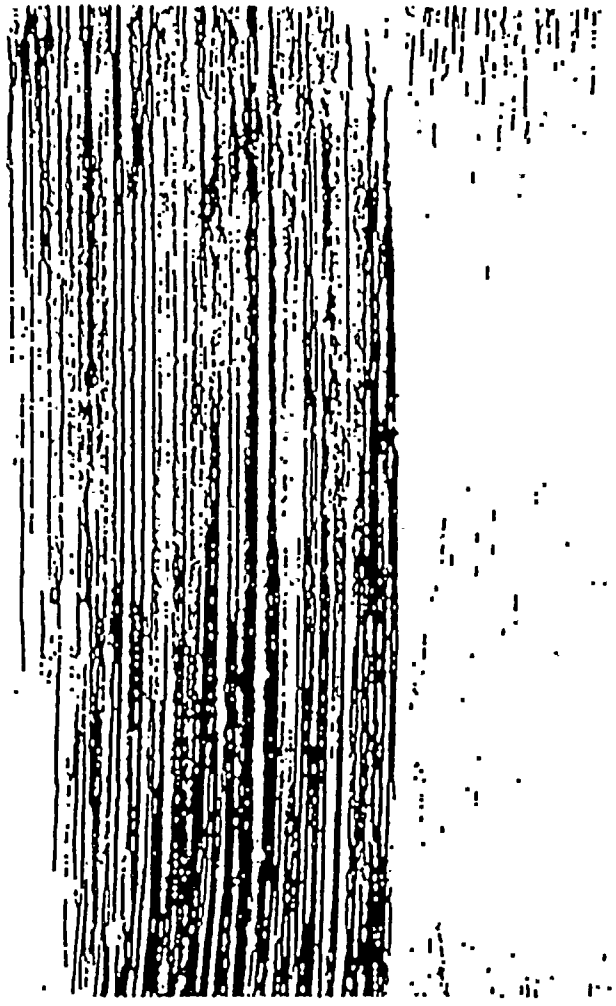

Fig. 6. Wear track on chromium plated Inconel.
Slider material was Inconel - Test 38
Load - 1500 psi
Lubricant - Deoxygenated water
Temperature - 200 F
Period - 2000 cycles

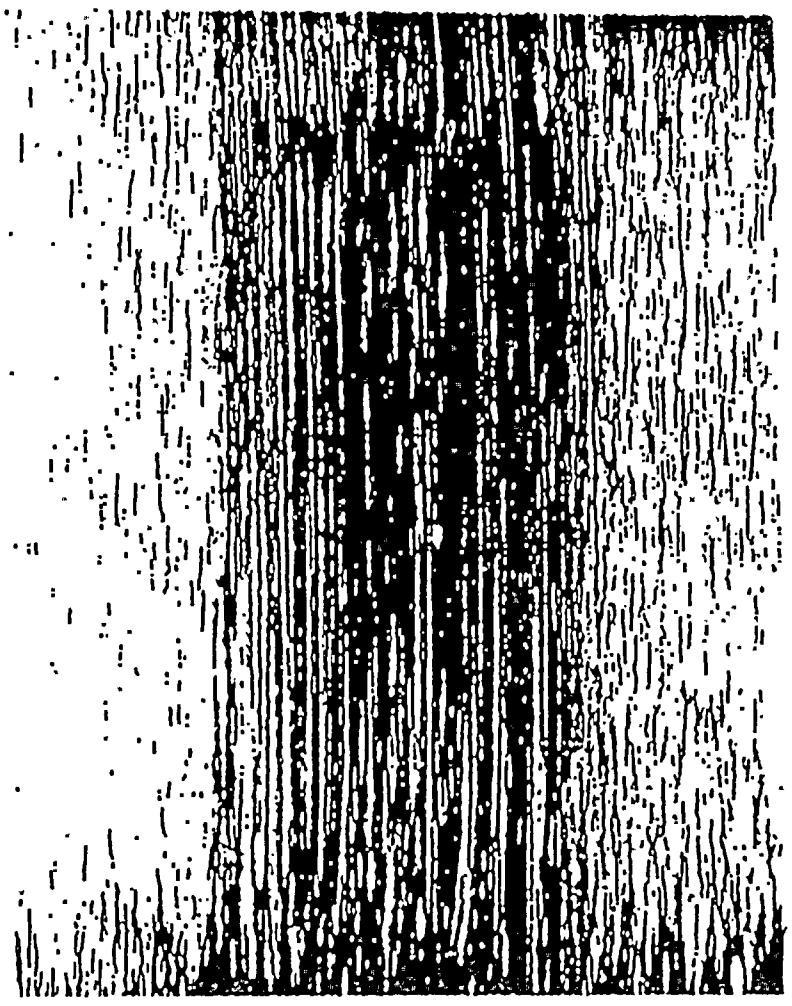

Fig. 7. Wear track on chromium plated 304 Stainless Steel. Slider was 304 Stainless Steel - Test 40.
Load - 1500 psi
Lubricant - Deoxygenated water
Temperature - 200 F
Period - 2000 cycles

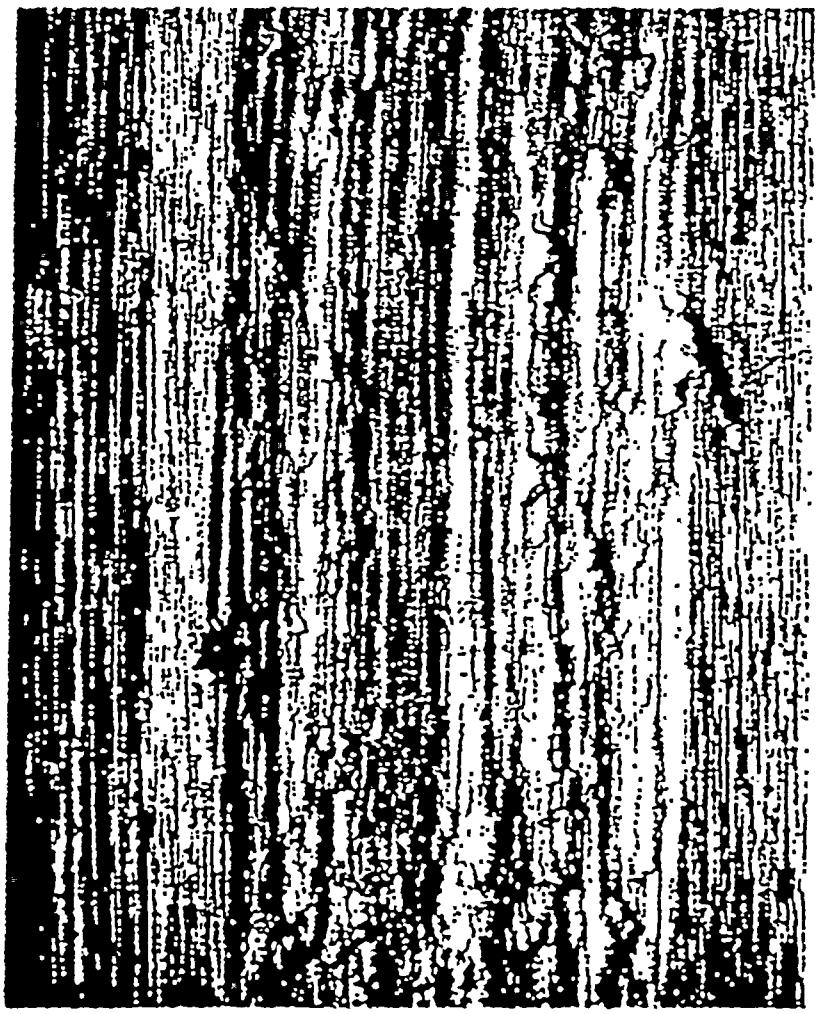

Fig. 8. Wear track observed on electrolized Inconel. Slider was Inconel - Test 36.

Load	- 1500 psi
Lubricant	- Dry
Temperature	- 74 F
Period	- 500 cycles (suspended test)

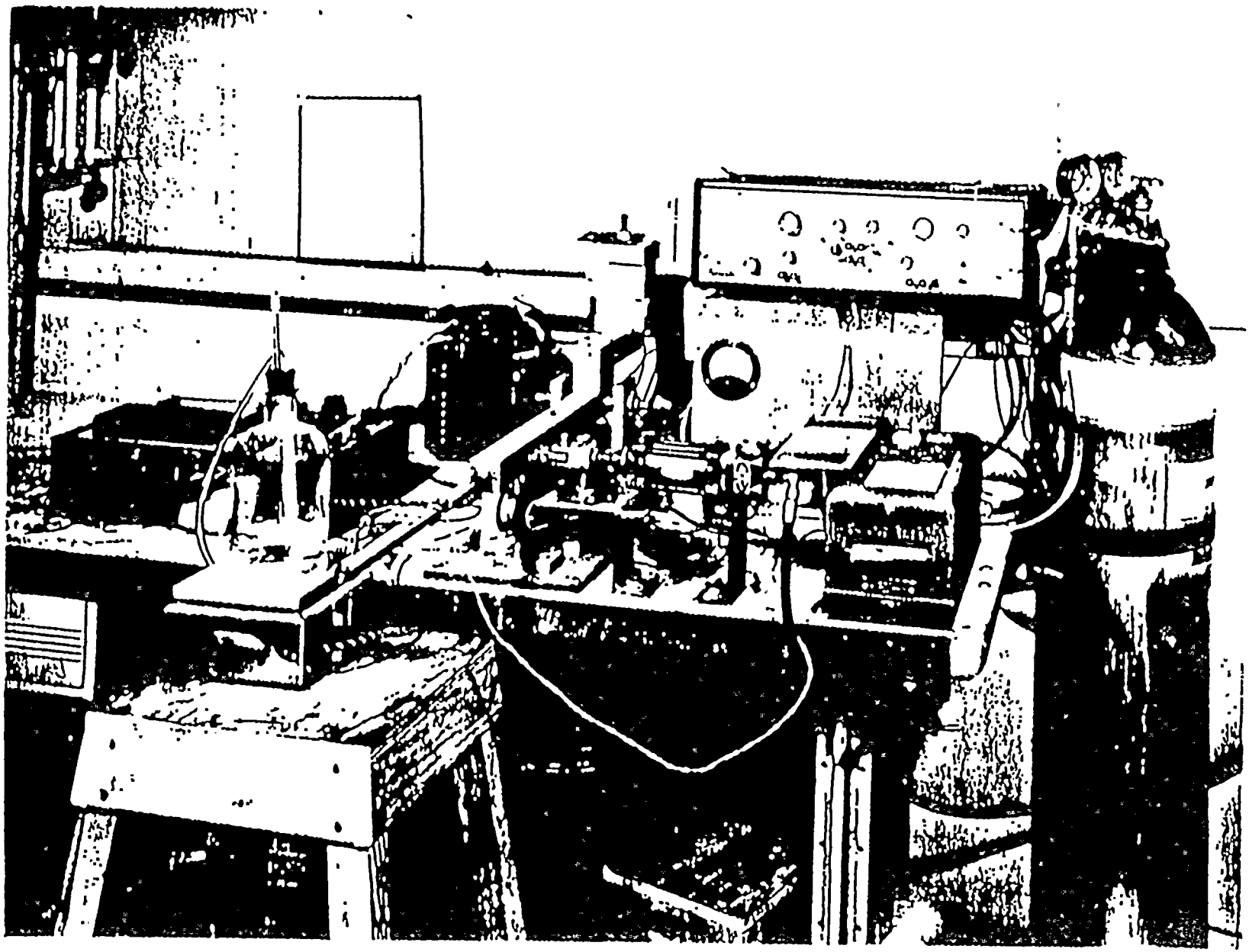

Fig. 9. Wear test apparatus.

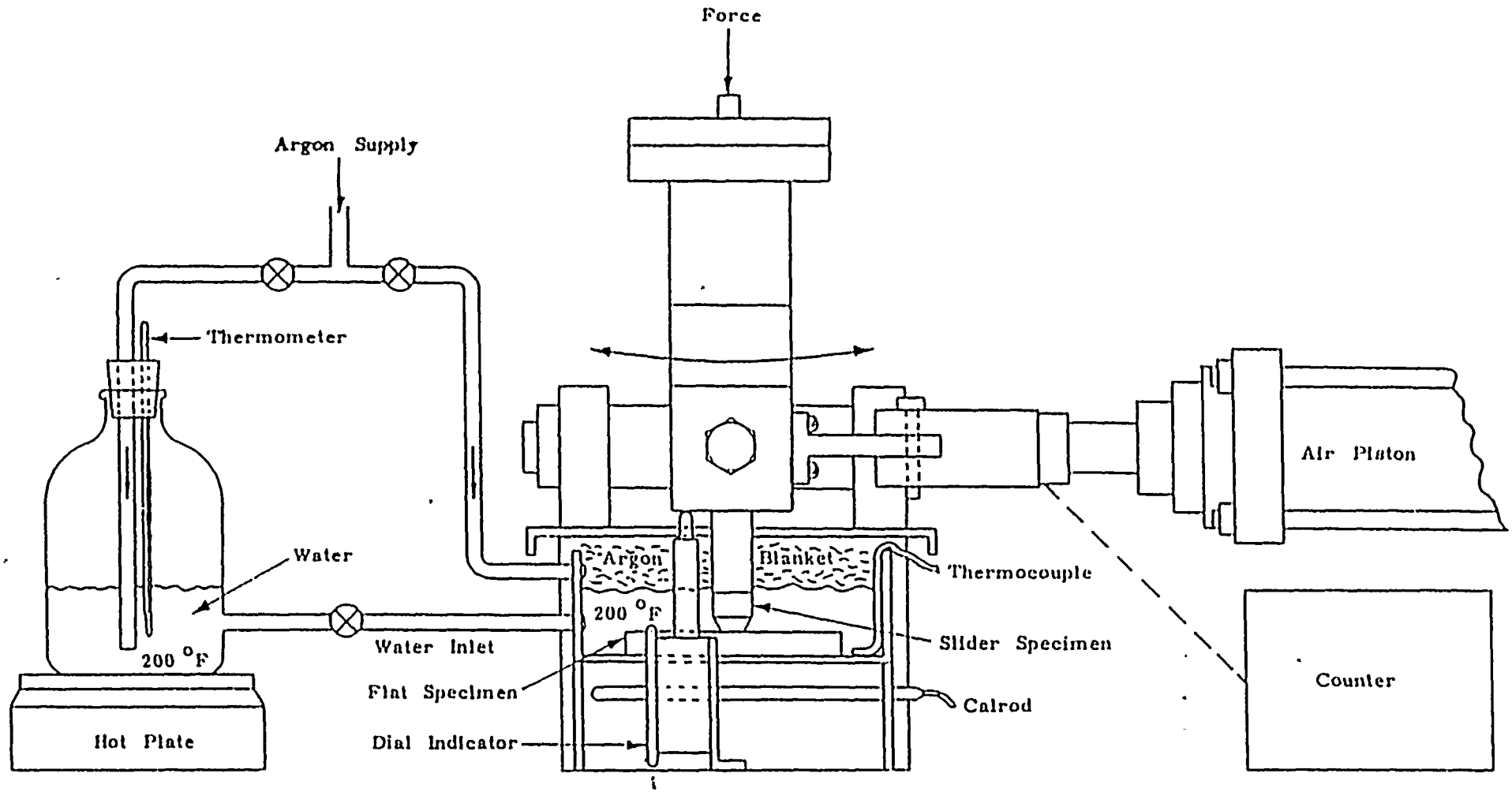

Fig. 10. Schematic diagram - Front view of wear test apparatus.

GENERAL ELECTRIC

General Engineering Laboratory

SCHENECTADY, NEW YORK

TECHNICAL INFORMATION SERIES

AUTHOR	SUBJECT CLASSIFICATION	NO.
R.E. Lee, Jr.	Friction and Wear of Structural Materials	60GL20
		DATE 1/22/60

TITLE: Investigation of the Sliding Behavior of a Number of Alloys Under Dry and Water Lubricated Conditions

ABSTRACT

An investigation was made to determine the sliding characteristics of a number of alloys under consideration for use as components in a pressurized reactor. The materials were studied under dry sliding (74 F), and water lubricated conditions (200 F).

G.E. CLASS	REPRODUCIBLE COPY FILED AT LIBRARY OF GENERAL ENGINEERING LABORATORY SCHENECTADY, NEW YORK	NO. PAGES
I		14
GOV. CLASS.		

CONCLUSIONS

Under the conditions tested:

1. The wear and surface damage of Inconel sliding against itself was considerably more severe than the austenitic AISI 304 stainless steel in combination with itself.
2. Replacing one of the Inconel-Inconel sliding members with Zircaloy 2, significantly reduced the wear and surface damage.
3. The application of protective coatings resulted in considerable improvement over that of the conventional (uncoated) material combinations. The coatings that proved effective in reducing the wear and surface damage of Inconel were: a. Stellite 6 (overlay), b. Colmonoy 6 (overlay), c. Hard Chromium Plate

INFORMATION PREPARED FOR Knolls Atomic Power Laboratory

TESTS MADE BY Roy Christie

AUTHOR R. E. Lee, Jr. R.E. Lee Jr.

COUNTERSIGNED H. Apkarian H. Apkarian

COMPONENT Bearing and Lubricant Center, General Engineering Laboratory

GL-14-C

GENERAL ELECTRIC

General Engineering Laboratory

SCHENECTADY, NEW YORK

DISTRIBUTION LIST — COMPLETE REPORT — TIS REPORT NO. 60GL20

AIRCRAFT NUCLEAR PROPULSION DEPARTMENT, CINCINNATI, OHIO

D. T. Barry
W. G. Evans
T. Hunter
L. Kasbaum
W. V. Leeburn, P.O. Box 2147, Idaho Falls, Idaho
W. A. McDonald
B. J. Serowick
C. Zapf

ATOMIC POWER EQUIPMENT DEPARTMENT, SAN JOSE, CALIFORNIA

B. F. McClintic 300-76

CANADIAN GENERAL ELECTRIC, PETERBOROUGH, ONTARIO

J. R. Dorsey	M and G Eng., Apparatus Department
D. B. Nazzer	Civilian Atomic Power Department
P. F. Phelan	M and G Eng., Apparatus Department
H. G. Taylor	Civilian Atomic Power Department
B. Turner	Civilian Atomic Power Department

GENERAL ENGINEERING LABORATORY, SCHENECTADY, NEW YORK

H. Apkarian (3)	37-1020
W. A. Boothe	37-304
W. J. Cox	37-2051
J. E. Lake	37-631
R. E. Lee (6)	37-1020
E. L. Lustenader	37-611B
G. Sittner	37-351
L. Smith	37-304
Library	5-4
Reproducible	

HANFORD ATOMIC PRODUCTS DEPARTMENT, RICHLAND, WASHINGTON

H. W. Heacock Bldg. 762
J. V. Lawler

GENERAL ELECTRIC

General Engineering Laboratory

SCHENECTADY, NEW YORK

DISTRIBUTION LIST — COMPLETE REPORT (cont.) — TIS REPORT NO. 60GL20

KNOLLS ATOMIC POWER DEPARTMENT, SCHENECTADY, NEW YORK

C. F. Barrett	A1 - 113
J. Childs	P1 - 219
J. Dunbar	P3 - 191
W. Fleishmann (10)	P3 - 172
G. Hill	A1 - 226
E. H. Hull	2A44
J. F. Kagay	P3 - 161
A. S. Kerr	C2 - 111
B. S. Kosut	P2 - 140
H. Norden	D2 - 114
R. H. Oberdick	C3 - 129
H. Suss	P3 - 191
J. L. Vanullen	A1 - 113

MEDIUM AC MOTOR DEPARTMENT, SCHENECTADY, NEW YORK

E. R. Booser	50-312
J. J. Broderick	81-2nd floor
D. A. Smeaton	50-312

SMALL STEAM TURBINE DEPARTMENT, FITCHBURG, MASSACHUSETTS

W. J. Caruso	4-3
A. E. Truran	

GENERAL ELECTRIC

General Engineering Laboratory

SCHENECTADY, NEW YORK

DISTRIBUTION LIST TITLE PAGE ONLY TIS REPORT NO. 60GL20

AIRCRAFT ACCESSORY TURBINE DEPARTMENT, LYNN, MASSACHUSETTS

J. F. Austin	1-46
T. Larkin	3-74
J. J. O'Connor	3-74

APPLIANCE MOTOR DEPARTMENT, DE KALB, ILLINOIS

C. W. Otto

AIR CONDITIONER DEPARTMENT, LOUISVILLE, KENTUCKY

M. Kosfeld

AUTOMATIC BLANKET AND FAN DEPARTMENT, BRIDGEPORT, CONN.

J. O. McLean	21-EE

DIRECT CURRENT MOTOR AND GENERATOR DEPARTMENT, ERIE, PA.

G. D. Bradley
M. W. Kitzmiller

CAPACITOR DEPARTMENT, HUDSON FALLS, NEW YORK

H. H. Doetsch, Jr.	10-4

FLIGHT PROPULSION LABORATORY DEPARTMENT, CINCINNATI, OHIO

R. Brooks	
E. N. Bamberger	200
S. Drabek	
E. K. Martin	
J. R. Shaw	Malta Test Station
J. B. Wood	200

GEAR MOTOR AND TRANSMISSION DEPARTMENT, PATERSON, NEW JERSEY

J. A. Kohn	845 E. 25th Street

GENERAL ELECTRIC

General Engineering Laboratory

SCHENECTADY, NEW YORK

DISTRIBUTION LIST — TITLE PAGE ONLY (cont.) — TIS REPORT NO. 60GL20

GAS TURBINE DEPARTMENT, SCHENECTADY, NEW YORK

A. N. Smith	53-414

GENERAL ENGINEERING LABORATORY, SCHENECTADY, NEW YORK

R. O. Fehr	37-311
L. G. Gitzendanner	37-317

GENERAL PURPOSE CONTROL DEPARTMENT

W. E. Birchard	Bloomington, Illinois
E. R. Cummingham	Fort Wayne, Indiana
J. C. Fomenko	Bloomington, Illinois

HEAVY MILITARY PRODUCTS DEPARTMENT, SYRACUSE, NEW YORK

J. H. Wynn	4-26

HOME LAUNDRY DEPARTMENT, LOUISVILLE, KENTUCKY

M. J. Barnstead	
J. E. Rhodes	1-220

HOTPOINT HOME LAUNDRY DEPARTMENT, CHICAGO, ILLINOIS

J. S. Houston

HIGH VOLTAGE SWITCHGEAR DEPARTMENT, PHILADELPHIA, PA.

J. A. Oppel	4A-2
R. B. Shores	

HOUSEHOLD REFRIGERATOR DEPARTMENT, LOUISVILLE, KENTUCKY

R. L. Hadley	AP5-249
T. A. McGrew	AP5-239

GENERAL ELECTRIC

General Engineering Laboratory

SCHENECTADY, NEW YORK

DISTRIBUTION LIST TITLE PAGE ONLY (cont.) TIS REPORT NO. 60GL20

INSTRUMENT DEPARTMENT, LYNN, MASSACHUSETTS

R. S. Norman
J. A. Warburton

JET ENGINE DEPARTMENT, CINCINNATI, OHIO

M. F. Grandey	501
C. C. Moore	
T. W. Sproull	

LARGE MOTOR AND GENERATOR DEPARTMENT, SCHENECTADY, N.Y.

T. C. Johnson	41-303
P. Moench	41-303

LARGE STEAM TURBINE AND GENERATOR DEPARTMENT, SCHENECTADY, NY

A. C. Bahr	273-217
G. V. Browning	7-207
J. A. Owczarek	285-129
E. E. Zwicky, Jr.	273-360

LAMP DIVISION, CLEVELAND, OHIO

V. L. Beswick	Nela Park
W. D. Evans	Nela Park
J. Udouich	1133 East 152nd Street

LIGHT MILITARY EQUIPMENT DEPARTMENT,

R. G. Carson	Ithaca, New York
L. W. Furman	Johnson City, New York
B. W. Hayer	Ithaca, New York
F. V. Johnson	28-400, Schenectady

LOW VOLTAGE SWITCHGEAR DEPARTMENT, PHILADELPHIA, PA.

R. Baskerville
P. C. Netzel

GENERAL ELECTRIC

General Engineering Laboratory

SCHENECTADY, NEW YORK

DISTRIBUTION LIST TITLE PAGE ONLY (cont.) TIS REPORT NO. 60GL20

LOCOMOTIVE CAR AND EQUIPMENT DEPARTMENT, ERIE, PA.

R. W. Avery	1-14
C. Simon	5-6

MANUFACTURING SERVICES, SCHENECTADY, NEW YORK

B. F. Hart	10-1st Floor

MEDIUM AC MOTOR DEPARTMENT, SCHENECTADY, NEW YORK

P. Cochran	40-547
J. Cothren	46-1
R. M. Fisher, Jr.	40-528

METER DEPARTMENT, SOMERSWORTH, NEW HAMPSHIRE

F. W. Truesdell

MSTG AND G DEPARTMENT, LYNN, MASSACHUSETTS

M. Cohen	2-41A
C. B. Reilly	2-41A
G. F. Wolfe	2-41A

ORDNANCE DEPARTMENT, PITTSFIELD, MASSACHUSETTS

D. F. Haywood	OP 2
L. G. Hoag	
R. L. Hunter	

SMALL INTEGRAL MOTOR DEPARTMENT, FORT WAYNE, INDIANA

R. L. Sieber

SPECIALTY CONTROL DEPARTMENT, WAYNESBORO, VIRGINIA

J. K. Snell
C. Dixon

GENERAL ELECTRIC

General Engineering Laboratory

SCHENECTADY, NEW YORK

DISTRIBUTION LIST TITLE PAGE ONLY (cont.) TIS REPORT NO. 60GL20

SPECIALTY MOTOR DEPARTMENT, FORT WAYNE, INDIANA

L. R. Allendorph	18-3
R. W. Dochterman	18-3
M. D. Tupper	18-3

POWER TRANSFORMER DEPARTMENT, PITTSFIELD, MASSACHUSETTS

E. F. Bagdonas	

ROOM AIR CONDITIONER DEPARTMENT, LOUISVILLE, KENTUCKY

P. J. Dellario	6-244D

SEMICONDUCTOR PRODUCTS DEPARTMENT, SYRACUSE, NEW YORK

J. Larrison	6-228, Electronics park

SMALL AIRCRAFT ENGINE DEPARTMENT, LYNN, MASSACHUSETTS

E. G. Jackson	1000 Western Avenue
S. X. Karidas	2-45, River Works

VACUUM CLEANER DEPARTMENT, CLEVELAND, OHIO

A. G. Ostrognai	1734 Ivanhoe Road

ENCLOSURE 1